



저작자표시-비영리-변경금지 2.0 대한민국

이용자는 아래의 조건을 따르는 경우에 한하여 자유롭게

- 이 저작물을 복제, 배포, 전송, 전시, 공연 및 방송할 수 있습니다.

다음과 같은 조건을 따라야 합니다:



저작자표시. 귀하는 원저작자를 표시하여야 합니다.



비영리. 귀하는 이 저작물을 영리 목적으로 이용할 수 없습니다.



변경금지. 귀하는 이 저작물을 개작, 변형 또는 가공할 수 없습니다.

- 귀하는, 이 저작물의 재이용이나 배포의 경우, 이 저작물에 적용된 이용허락조건을 명확하게 나타내어야 합니다.
- 저작권자로부터 별도의 허가를 받으면 이러한 조건들은 적용되지 않습니다.

저작권법에 따른 이용자의 권리는 위의 내용에 의하여 영향을 받지 않습니다.

이것은 [이용허락규약\(Legal Code\)](#)을 이해하기 쉽게 요약한 것입니다.

[Disclaimer](#)

**February 2017**

**Ph.D. Dissertation**

**53BP1 regulates histone acetylation  
through interaction with  
ATP-Citrate-Lyase**

**Graduate School of Chosun University**

**Department of Biomedical sciences**

**Wu TingTing**

**53BP1 regulates histone acetylation  
through interaction with  
ATP-Citrate-Lyase**

53BP1에 의한 히스톤아세틸화 기전 연구

24<sup>th</sup> February 2017

**Graduate School of Chosun University**

**Department of Biomedical sciences**

**Wu TingTing**

**53BP1 regulates histone acetylation  
through interaction with  
ATP-Citrate-Lyase**

**Advisor: Prof. Ho Jin You**

A dissertation submitted to the Graduate School of Chosun  
University in partial fulfillment of the requirements for the de-  
gree of Doctor of Philosophy in Science

October 2016

**Graduate School of Chosun University**

**Department of Biomedical sciences**

**Wu TingTing**

**The Ph.D. dissertation of  
Wu TingTing is certified by**

**Chairman          Professor   In-Youb Chang \_\_\_\_\_**

**Committee Members:**

**Professor   Sang Pil Yoon \_\_\_\_\_**

**Professor   Tak bum Ohn \_\_\_\_\_**

**Professor   Jung-Hee Lee \_\_\_\_\_**

**Professor   Ho Jin You \_\_\_\_\_**

**December 2016**

**Graduate School of Chosun University**

## CONTENTS

<b>LIST OF FIGURES.....</b>	<b>05</b>
<b>LIST OF TABLES.....</b>	<b>06</b>
<b>ABSTRACT (IN KOREAN).....</b>	<b>07</b>
<b>I. INTRODUCTION.....</b>	<b>10</b>
 <b>II. MATERIALS AND METHODS</b>	
1. Plasmids.....	15
2. Additional antibodies.....	16
3. Cell culture.....	18
4. Mouse embryonic fibroblast cell isolation and MEF cell immortaliza- tion.....	19
5. ACL activity assay.....	20

6. Immunoprecipitation assay and Western blot.....	21
7. Cytoplasmic/Nuclear fraction and histone preparation.....	22
8. Production of GST fusion proteins.....	23
9. In vitro direct binding assay.....	23
10. Cell synchronization and Proliferation assay.....	24
11. Differentiation of 3T3-L1 adipocytes.....	25
12. Oil Red O Staining.....	26
13. Quantitative realtime PCR.....	26
14. Chromatin immunoprecipitation.....	27
15. Animals.....	28
16. Analysis of cholesterol and triglyceride.....	29
17. Immunohistochemistry.....	30

18. mtDNA damage assay .....	30
19. Immunofluorescence microscopy .....	31
20. DNA fiber assay .....	31

### III. RESULTS

1. 53BP1 interacts with ACL .....	34
i. ACL; Novel binding protein of 53BP1 .....	34
ii. Binding of 53BP1 and ACL in both of vitro and vivo .....	36
iii. The N-terminal region of 53BP1 mediates the interaction with ACL .....	41
2. 53BP1 regulates ACL activity .....	46
3. Mice deficient in 53BP1 exhibit decreased body weight and fat formation .....	50
4. 53BP1 regulates histone acetylation .....	55

i.	Deletion of 53BP1 leads to decreased histone acetylation.....	55
ii.	53BP1 regulates histone acetylation in the response of serum stimulation and glucose condition.....	63
iii.	53BP1 regulates histone acetylation during adipocyte differentiation.....	67
iv.	53BP1 regulates histone acetylation during mouse spermatogenesis.....	74
5.	53BP1 influence gene expression through histone acetylation.....	79
6.	Novel functions of 53BP1 by histone acetylation mediated gene expression decrease.....	96
i.	Downregulation of Dna2 in 53BP1-deficient cells.....	96
ii.	Decrease of plk4 in 53BP1-deficient cells.....	97
iii.	Reduction of MCM3 and MCM7 in 53BP1-knockdown cells.....	98

**IV. DISCUSSIONS.....104**  
**REFERENCES.....112**  
**ABSTRACT (IN ENGLISH).....121**

**CONTENTS OF FIGURES**

Figure 1. ATP citrate lyase regulates the flow of glucose carbons to cytosolic acetyl-CoA during glucose catabolism.....11  
 Figure 2. The two major mammalian pathways for ACL enzyme.....14  
 Figure 3. 53BP1 as a ACL- associated protein.....35  
 Figure 4. Binding of 53BP1 and ACL in both of vitro and vivo.....39  
 Figure 5. Identification of a ACL Binding site/domain in 53BP1.....45  
 Figure 6. 53BP1 regulates ACL activity.....48  
 Figure 7. Deficiency in 53BP1 results in mice physiologic data and lipid metabo-

lism.....53

Figure 8. 53BP1 is important for maintenance of histone acetylation.....59

Figure 9. 53BP1 regulates histone acetylation in cell cycle and glucose-dependent.....63

Figure 10. Silencing 53BP1 reduced histone acetylation in adipocytes.....69

Figure 11. Testicular development and spermatogenesis in 53BP1 knockout mice.....74

Figure 12. 53BP1 influence gene expression through control histone acetylation.....83

Figure 13. Preparatory experiments of 53BP1 new functions.....95

## CONTENTS OF TABLES

Table 1. Physiologic date of 53BP1 wild and knockout type mice.....52

Table 2. Deep sequencing data of 53BP1 wild and knockout type cells.....81

Table 3. Oligonucleotide pimer of the mRNA real-time PCR.....89

Table 4. Promoter primer of the chip assay.....93

## 국문초록

### 53BP1에 의한 히스톤아세틸화 기전연구

Wu TingTing (오정정)

지도교수 : 유호진

조선대학교 일반대학원

의과학과

유전자 손상 반응의 중요 조절자인 53BP1이 대사 효소인 ACL과 결합함을 yeast two hybrid assay를 통해 처음으로 동정하여, 53BP1에 의한 ACL효소 활성 조절 기전을 확인하였다. ACL 효소는 미토콘드리아와 세포질내의 아세틸 CoA 조절을 통해서 지질대사과 포도당 대사에 중요한 역할을 차지할뿐만 아니라 세포핵내 아세틸 CoA 조절을 통해 히스톤 아세틸레이션에 중요한 역할을 한다고 보고되어 있다.

히스톤 변형, 즉 히스톤 아세틸화는 DNA메틸화와 함께 DNA의 염기서열에는 변화가 일어나지 않은 상태에서 유전자의 발현을 조절하는 가장 핵심적인 후천적 기작

이다. 53BP1과 효소인 ACL의 상호작용확인하기 위해 먼저 in vivo와 in vitro에서 53BP1과 ACL의 결합을 면역침강법을 통해 확인하였다. 특히 53BP1 N-terminal부위가 ACL과의 결합에 중요함을 확인하였고 이부분 결합에 통하여 ACL효소의 활성화에 영향을 미친다. 이어서 ACL 효소 활성조절을 통해 포도당대사와 연관성 확인하기 위해 동물실험을 진행하였다. 53BP1결핍된 마우스에서 지방합성이 감소된다는 것을 확인하였고 지방합성과정중에 중요한 genes ACC하고 FAS의 단백질 발현양이 감소되는 것 확인 할 수 있었다. 그다음에 53BP1의 히스톤 아세틸화와 연관성을 확인하기 위하여 실험진행하였다. 히스톤 아세틸레이션의 변화를 확인하기 위해 실험을 4부분으로 진행하였다. 1. 일반상태에 세포내 히스톤 아세틸레이션의 변화. 2. 세포주기에 의하여 히스톤 아세틸레이션의 변화. 3. 지방전구세포에서 지방세포로 분화되는 adipogenesis과정에서 히스톤 아세틸레이션의 변화, 몇 상관 gene의 발현. 4. Mouse 모델에서 testis의 development의 정도을 통해 히스톤 아세틸레이션의 변화확인하였다. 4부분 실험은 모두다 53BP1 gene 존재하거나 결핍한 상태에서 비교해서 진행하였으나 53BP1 gene결핍한 상태에서 히스톤 아세틸화 감소된다는 것을 확인 할 수 있었다.

이어서 히스톤 아세틸레이션 조절을 통해 gene expression을 어떻게 조절하는지에 대한 연구도 진행하였다.

결론적으로 ACL은 세포에 Acetyl-CoA를 공급하는 효소로 53BP1이 세포 내ACL효소 활성조절을 통해 히스톤의 아세틸화를 조절함으로써 gene expression 영향을 미치며 53BP1의 세포내 새로운 기능을 확인하였다.

## INTRODUCTION

Metabolic syndrome refers to a group of metabolic disturbances, including obesity, hyperglycemia, dyslipidemia and hypertension, which increase the risks for cardiovascular disease, diabetes and stroke [1]. Glucose is a major energy source for the body to cope with nutrient deprivation. ACL enzymatic activity is poised to affect both glucose-dependent lipogenesis and cellular bioenergetics (Figure 1) [2]. ACL cleavage of cytosolic citrate generates acetyl-CoA and oxaloacetate. Acetyl-CoA is the precursor for the synthesis of fatty acids, cholesterol, and isoprenoids, while oxaloacetate is reduced to malate, using NADH as an electron donor [3]. ACL as a lipogenic enzyme is also present in the nucleus and plays a crucial role in regulating nuclear acetylation events, including histone acetylation [4]. Acetyl-CoA is a key intermediate in three major metabolic pathways (Figure 2). ACL converts citrate to acetyl-CoA. In the nucleus, acetyl-CoA serves as a substrate for histone acetyltransferases (HATs) that modify histones with acetate to affect the transcription of key metabolic genes. In the cytosol, acetyl-CoA supports lipid synthesis [5].

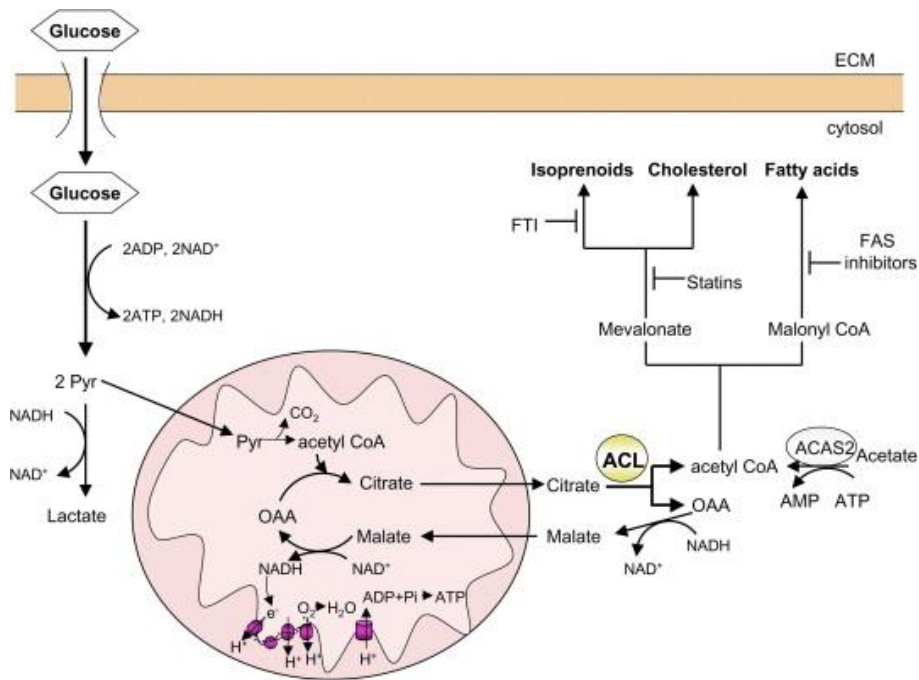


**Figure 1. ATP citrate lyase regulates the flow of glucose carbons to cytosolic acetyl-CoA during glucose catabolism. (Georgia Hatzivassiliou etc., Cancer Cell., 2005).**

Chromatin is the central component of the nuclear landscape that controls the expression of genes, which regulate stem cell pluripotency and ability to differentiate into specialized cell types that compose tissues and organs of multicellular organisms [6]. The basic unit of chromatin is the nucleosome, which consists of a segment of duplex DNA wrapped around a histone octamer comprised of two of each of the conventional histone proteins: H2A, H2B, H3, and H4. Histones,

the building blocks of mammalian chromatin, are small basic proteins that can be covalently modified by methylation, acetylation, phosphorylation; ubiquitination etc [7], [8], [9]. First reported histone acetylation in 1964 [10]. Histone acetylation can be dynamically regulated by several classes of histone deacetylases (HDACs) and families of histone acetyltransferases (HATs) [11]. HATs are classified into two groups, HAT A and HAT B. HAT A family are found in the nucleus, where they transfer the acetyl group from Acetyl-CoA to an  $\epsilon$ -NH<sub>2</sub> group of histone N-tails after the assembly into nucleosomes [12], [13]. HAT B family act in the cytoplasm and transfer the acetyl group from Acetyl-CoA to an  $\epsilon$ -NH<sub>2</sub> group of free histones prior to their deposition on the DNA [14].

The DNA damage response factor 53BP1 functions at the intersection of two major double strand break (DSB) repair pathways – promoting nonhomologous end-joining (NHEJ) and inhibiting homology-directed repair (HDR) [15], [16], [17]. Recently, some reports identified 53BP1 and USP28 as essential components acting upstream of p53 to mediate the stress response not only to centrosome loss, but also to other distinct defects that cause prolonged mitosis [18]. Although,

53BP1 repair pathways entirely different from ACL metabolism pathways. Through 53BP1 interacting protein yeast two-hybrid screening we found that 53BP1 interacts with ACL, and 53BP1 deficient cells showed decrease ACL activity. Based on ACL's potential role in the integration of glucose and lipid metabolism. We have assessed if 53BP1 through regulate the activity of ACL to affect glucose-dependent lipogenesis. We investigated the metabolic effects used 53BP1 wild type and knockout mice. The physiologic data were compared between 53BP1 WT and KO type mouse and lipid metabolism gene expression were measured. We also indicated that 53BP1 can regulates ACL-dependent histone acetylation at various conditions, and through control histone acetylation effect to gene expression, and affect glucose-dependent lipogenesis. New functions of 53BP1 was being reported.

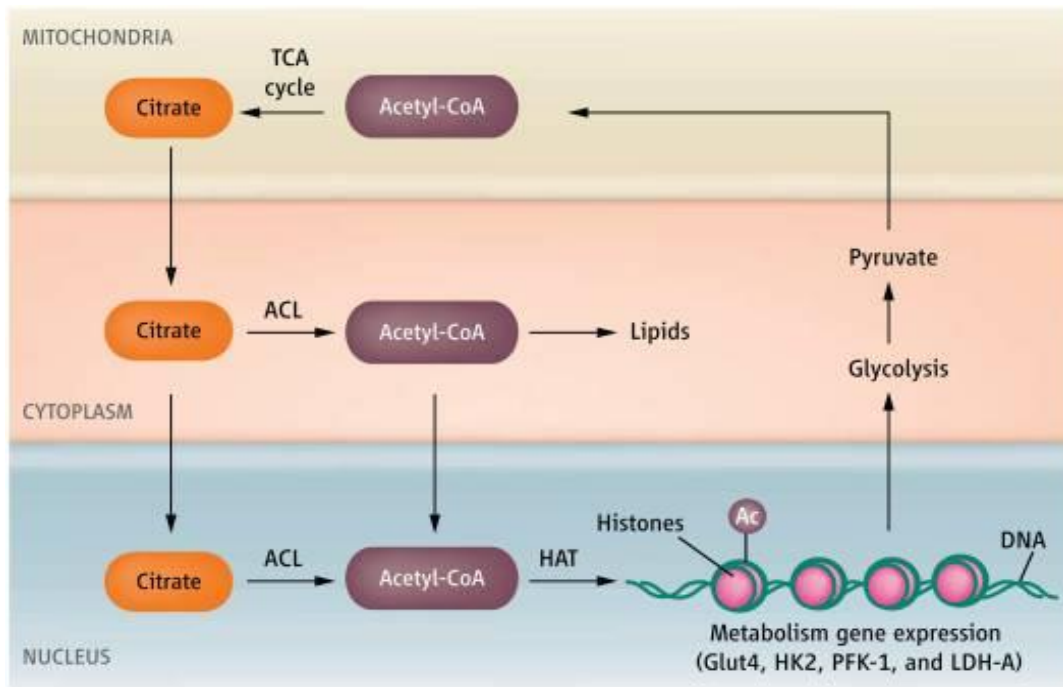


**Figure 2. The two major mammalian pathways for ACLy enzyme (Jeffrey C. Rathmell and Christopher B. Newgard. 2009).**

## MATERIALS AND METHODS

### 1. Plasmids

The full-length ACL cDNA was amplified from HELA cell by RT-PCR using the ACL primers 5'-CAT AAG CTT ATG TCG GCC AAG GCA ATT TCA-3 (sense) and 5'-TAA CCG CGG TTA CAT GCT CAT GTG TTC CGG-3' (anti- sense). The amplified ACL cDNA construct was cloned into the mammalian expression vector pEGFP-N1 in-frame with the GFP tag. The ACL sequence was confirmed by automated DNA sequencing. The 53BP1 full construct is from addgene and other constructs N1 (a.a 1-699), N2 (a.a 1-500), N3 (a.a 1-300), N4 (a.a 1-100), N5 (a.a 101-699), N6 (a.a 301-699), N7 (a.a 501-699), N8 (a.a 101-300) prepared in our laboratory. The amplified 53BP1 construct was cloned into the mammalian expression vector pcDNA3 in frame with the hemagglutinin (HA) tag and using the primers N1-N4\_53BP1-5'- TCC CTC GAG CCT GGG GAG CAG ATG GAC CCT-3'(sense), N1\_53BP1-5'-TGA GGG CCC AGT CAG AGA AAG GTG CAA CGG A-3'(antisense), N2\_53BP1-5'- TAA GGG CCC AAT CTC TGA AGT TTT AGA ACA CTC-3'(antisense), N3\_53BP1-5'- GGT GGG CCC TGG TGA

CTT CTG AAT CTG CAG TC-3' (antisense), N4\_53BP1-5'-AGA GGG CCC AGA ATC CAC  
AGG GTC TGC AAC C-3'(antisense). N5-N7\_ 53BP1-5'-TGA GGG CCC AGT CAG AGA  
AAG GTG CAA CGG A-3' (antisense), N5\_53BP1-5'-ACC CTC GAG TAA CTT GGA CAC  
ATG TGG TTC-3' (sense), N6\_53BP1-5'-AAT CTC GAG CCA CTC CTG CCA CCA CTC  
TGC -3' (sense), N7\_53BP1-5'- GCC CTC GAG ATG GAG AAA ACA CAC AGA TTG-  
3'(sense), N8\_53BP1-5'- TAA GGG CCC TCA CAA AAC CTC AGG CTC-3'(antisense).

## 2. Additional antibodies

The following antibodies were used for immunoprecipitations : Rabbit polyclonal anti-53BP1 (sc-22760, Santa Cruz Biotechnology, 1 $\mu$ g), Rabbit monoclonal anti-ACL (NB110-55476, NOVUS Biologicals, 1:200), Rabbit polyclonal anti-HA-probe (sc-805, Santa Cruz Biotechnology, 1 $\mu$ g), Rabbit polyclonal anti-GFP (sc-8334, Santa Cruz Biotechnology, 1 $\mu$ g). Immunoblotting were performed using Rabbit polyclonal anti-53BP1 (TA309918, Origene, 1:1000) for mouse cell line, Mouse anti-53BP1 (612523, BD Transduction Laboratories, 1:1000) for human cell line,

Rabbit monoclonal anti-ACL (NB110-55476, NOVUS Biologicals, 1:4000), Mouse monoclonal anti- $\alpha$ - Tubulin ( LF-MA0117, Abfrontier, 1:4000), Mouse monoclonal anti-acetylated  $\alpha$ -Tubulin (sc-23950, Santa Cruz, 1:2000), Mouse monoclonal anti- $\beta$ -actin (sc-47778, Santa Cruz, 1:4000), Mouse monoclonal anti-HA-probe (sc-7392, Santa Cruz, 1:1000), Mouse monoclonal anti-GFP (sc-9996, Santa Cruz, 1:1000), Rabbit monoclonal anti-PPAR- $\gamma$  (#2443, Cell Signaling, 1:1000), Rabbit polyclonal anti-C/EBP  $\alpha$  (#2843, Cell Signaling, 1:1000), Mouse monoclonal anti-Glut4 (#2213, Cell Signaling, 1:1000), Rabbit monoclonal anti-Hexokinase II (#2867, Cell Signaling, 1:1000), Rabbit polyclonal anti-PFK-1 (H00005213-D01P, NOVUS, 1:1000), Rabbit polyclonal anti-LDHA (#2012, Cell Signaling), Rabbit polyclonal anti-Histone H3 (ab1791, Abcam, 1:5000), Rabbit polyclonal anti-Histone H4 (ab7311, Abcam, 1:1000), Rabbit polyclonal anti-Histone H2A (ab18255, Abcam, 1:500), Rabbit polyclonal anti-Histone H2B (ab1790, Abcam 1:4000), Rabbit polyclonal anti-acetyl-Histone H3 (06-599, Millipore, 1:2000), Rabbit polyclonal anti-acetyl-Histone H4 (06-866, Millipore, 1:4000), Rabbit polyclonal anti-acetyl-Histone H2B (07-373, Millipore, 1:1000) and Lysine specific Histone acetylation used

sample Kits – Acetyl-Histone H3 (#9927, Cell Signaling, 1:1000), Acetyl-Histone H4 (#8346, Cell Signaling, 1:1000), Acetyl-Histone (#9933, Cell Signaling, 1:1000). Rabbit polyclonal anti-ACC (#3662S, Cell Signaling, 1:1000), Mouse monoclonal anti-FAS (610962, BD Biosciences, 1:1000).

### 3. Cell culture

The human cervix adenocarcinoma cell line HeLa, human osteosarcoma bone morphogenetic cell line U2OS and human embryonic kidney cell line HEK293T, mouse cell line preadipocyte cell 3T3-L1, Mouse embryonic fibroblast cell line (primary and immortalize) were cultured in Dulbecco's modified Eagles's medium. HCT116 cell were cultured in Iscove's modified Dulbecco's medium. A549 cell were cultured in RPMI 1640 media. In all cases, the media was supplemented with 10% heat-inactivated fetal bovine serum (Cambrex Corp., East Rutherford, NJ, USA), 100unit/ml penicillin and 100mg/ml streptomycin sulfate (Invitrogen, Carlsbad, CA, USA). Particularly, 1X MEM non-essential amino acid solution (Sigma) was supplied for primary MEF cell. All cells were

maintained in a humidified incubator containing 5% CO<sub>2</sub> at 37°C. Upon reaching 70-80% confluency, cells were digested with 0.5% trypsin-EDTA before being passaged. Cells in exponential growth were harvested for subsequent experiments.

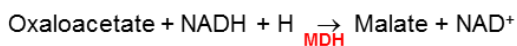
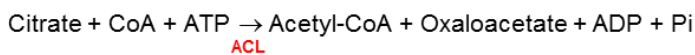
#### **4. Mouse embryonic fibroblast cell isolation and MEF cell immortalization**

Dissect mouse embryos 13.5 days and wash embryos 3 times with PBS, then remove head and internal organs from each embryo. Then add 2mL full media and mince tissue for an additional few minutes until pieces are further reduced in size with single edge blades. Remove the minced tissue to 15mL tube and place tube at room temperature 5 minutes, then remove the supernatant and add trypsin mixture (collagenase: trypsin EDTA: free media = 1:4:5) 1-2mL to the pellet, vigorously pipette mixture up and down, then incubate the tube at 37°C water bath for 30minutes and invert the tube every 3-5 minutes. After 30 minutes, spin down tubes of cells 1500rpm for 10 minutes. Remove the gelatin and plate cells on to the 10cm dishes. These cells are passage 0 (p0). Change media next day.

Immortalization of MEF used SV40 T antigen. Split primary MEF at p3 into 6 well dishes. Transfect 50% confluent well with 2ug tag expression vector using Lipo2000, incubate cells 48hrs split them into a 10cm dish= P1. Split 1/10 at least 5 times, by P6-100,000 the cells should grow to confluence in ~3-4 days after a 1/10 split.

## 5. ACL activity assay

< ACL-MDH coupled method >



ACL activity was measured by the malate dehydrogenase coupled method as described previously [19]. Cell lysates were extracted from mouse and human cell lines and incubated with the reaction mixture (10mM Mgcl<sub>2</sub>, 100mM Tris-HCL PH 8.5, 20mM citrate, 0.33mM CoASH, 0.14mM NADH, 10mM DTT, 2.5mM ATP and 3.3U/mL MDH ) at 37°C for 10 minutes. ACL activity was measured every 5 minutes more than 2 hours using spectrophotometer.

## 6. Immunoprecipitation assay and western blot

Total protein of cell were lysed in RIPA buffer (50mM Tris-HCl (pH 7.5), 150mM NaCl, 1% NP-40, 0.5% sodium deoxycholate, 0.1% sodium dodecyl sulfate) with protease inhibitors (Roche Diagnostic Corp.). Snap-frozen tissues (20-50mg) were homogenized using BioMasher (Nippi, Incorporated Protein Engineering Office, Japan), and were added to RIPA Buffer, sonicating. After centrifugation at 15000rpm for 30min at 4°C, the supernatant were used.

Equal amounts of protein were separated by 6–15% SDS-PAGE followed by electrotransfer onto a polyvinylidene difluoride membrane (Millipore, Bedford, MA, USA). The membranes were blocked for 1 hrs. with TBS-t (10mM Tris-HCl (pH 7.4), 150mM NaCl and 0.1% Tween-20) containing 5% skim milk and then incubated at 4°C with primary antibodies. The blots were washed four times for 15 min with 0.1% Tween 20 containing TBS-t and then incubated for 2 hrs. with peroxidase-conjugated secondary antibodies (1:4000). The membranes were washed four more times and developed using an enhanced chemiluminescence detection system (ECL; GE Healthcare, Buckinghamshire, UK).

For the immunoprecipitation assays, aliquots of soluble cell lysates were precleared with protein A/G plus-agarose beads (Santa Cruz Biotechnology), G sepharose and A sepharose (GE Healthcare) as indicated and then incubated at 4 °C for 4h. Next, the appropriate antibody was added, and incubated at 4 °C for 12h. After the addition of fresh protein A/G plus-agarose bead, G sepharose and A sepharose, the reaction was incubated overnight at 4 °C with rotation. The beads were washed three times in RIPA buffer without protease inhibitors, resuspended in SDS sample buffer and boiled for 5 min. The samples were then analyzed by western blotting using the appropriate antibodies.

## **7. Cytoplasmic/Nuclear fraction and histone preparation**

Total protein were lysed cytosol extraction buffer (10mM HEPES (PH7.5), 3mM MgCl<sub>2</sub>, 14mM KCl, 5% glycerol, 1mM DTT), Incubate on ice for 10min. then add 0.2% NP-40 vortexing 10sec, and centrifugation at 8600g for 2min at 4 °C. Supernatant is cytoplasmic. Then wash pellet twice use cytosol extraction buffer. For nuclear fraction use buffer (10mM HEPES, 3mM MgCl<sub>2</sub>, 400mM NaCl, 5% glycerol, 1mM DTT), Incubate on ice for 30min, centrifugation maximum

30min. Histone extraction use a protocol from nature [20].

## 8. Production of GST fusion proteins

*E. coli* BL21 harboring the GST-53BP1 expression construct was grown in Luria broth (LB) culture supplemented with 100 µg/ml ampicillin and incubated overnight at 37 °C and 150 rpm. Fresh LB liquid (20 ml) containing 100 µg/ml ampicillin was incubated with 40ul of preculture and was incubated at 37 °C and 200 rpm to reach OD<sub>600</sub>:0.8. Then, the culture was induced with 1 mM IPTG and incubated at 37 °C with shaking at 200 rpm for 3hr. Cells were harvested at different time points after induction. The GST-53BP1 expression was evaluated on 10% SDS-PAGE and visualized using Coomassie-blue staining.

## 9. In Vitro direct binding assay

GST-tagged human 53BP1 fragments were expressed in bacteria and isolated with glutathione agarose beads. Bead-bound fragments (1 µg) were incubated with 200 ng purify ACL proein (Si-

no Biological Inc.) in 0.5 ml of binding buffer containing 20 mM TrisHCl, pH 7.5, 150 mM NaCl, 0.5% NP40, 1 mM EDTA, 1 mM DTT, and 10% glycerol at 4°C for 90 min. The beads were retrieved, washed, and subjected to immunoblotting and staining with Coomassie brilliant blue.

## 10. Cell synchronization and proliferation assays

Primary MEFs were seeded at  $5 \times 10^5$  in 10 cm dishes for 48 hours in media containing 10% FBS in DMEM. Following, cells were serum starved in 0.1% FBS for 16 hours, followed by mitogenic stimulation by serum shock with 50% horse serum (Gibco), and then continuous culture in 10% FBS in DMEM for the duration of the experiment. Cells were harvested for protein analysis every 3 hours by lysis with RIPA buffer and analyzed by Western blot. For glucose-dependence assays, siRNA-transfected MEFs were stripped of serum proteins by washing three times with 0.35% essentially fatty acid free bovine serum albumin (Sigma #A6003) and then cultured in the complete absence of serum for 16 hours. Cells were then exposed to 10% dialyzed FBS in DMEM in

the presence (25mM) or absence (0mM) of glucose and lysed in RIPA buffer at the indicated time points.

## **11. Differentiation of 3T3-L1 adipocytes**

3T3-L1 preadipocytes were transfected with CTL, 53BP1, or ACL siRNA. 2 days later, confluent cells were stimulated with 5 mM isobutylmethylxanthine, 1 uM dexamethasone, 10 ug/ml insulin. (all from Sigma) in DMEM with 10% FBS, to induce differentiation to adipocytes [21], [22]. Cells were treated with differentiation cocktail for 4 days (medium changed at day 2). For experiments lasting longer than 4 days, cells were placed into medium containing 10% FBS and insulin. Differentiation was performed in DMEM containing 25 mM glucose, except in experiments with variable glucose concentrations, in which case glucose-free DMEM (Invitrogen) was used and supplemented with the indicated amounts of D-glucose

## 12. Oil Red O staining

Working solution was generated by mixing 6 parts stock solution (Sigma O1391) with 4 parts H<sub>2</sub>O. Cells were washed in PBS and then fixed for 30 minutes at RT with 4% paraformaldehyde. Cells were then washed 2x in dH<sub>2</sub>O and 1x in 60% isopropanol and then stained in working solution for 30 min. Stain was then removed and cells washed 4x in dH<sub>2</sub>O.

## 13. Quantitative PCR analysis

Cell and tissue RNA was isolated in each condition using Trizol (Invitrogen). First-strand cDNA was synthesized with M-MLV reverse transcriptase and Oligo dT primers. Real-time quantitative PCR was done with the SYBR Green PCR system, using GAPDH as an internal control for normalization.

## 14. Chromatin immunoprecipitation

Chromatin immunoprecipitation assays were performed using the ChIP Assay Kit (Cell signaling # 9002). Primary MEF (P5) cell 53BP1 Wild type (WT) and Knockout (KO) type were used. DNA and histones were cross linked in 1% formaldehyde in culture media for 10 minutes, and then add 1X glycine. 100mm dish were used for each condition. After washing in cold PBS, cells were centrifuged and then lysed in 500ul buffer A (with DTT, PIC, and PMSF). Centrifugation on 3000rpm for 5min at 4°C. Remove the supernatant. Use 600ul buffer B (without DTT) washing the pellet, and then use buffer B (with DTT) 400ul resuspension and add 1ul Micrococcal nuclease incubation 20min at 37°C then add 0.5M EDTA to stop the reaction, Lysate was then sonicated to shear DNA to approximately 200-1000 bp. Samples were spun down and 100 µl of the supernatant used for each of triplicate immunoprecipitations with antibodies to AceH3 , and 1 replicate for normal rabbit IgG. Each sample was diluted 10x in ChIP dilution buffer and immunoprecipitations were performed overnight with above antibodies and protein A agarose. The next day, samples were washed in low salt immune complex buffer, high salt immune complex buffer, LiCl immune complex buff-

er, and TE buffer. Histone complexes were eluted in elution buffer (1% SDS, 100 mM NaHCO<sub>3</sub>).

Crosslinks were reversed by adding 10  $\mu$ l 5 M NaCl and incubating at 65°C for 30min. Samples were treated with proteinase K for 2 hour at 65°C, and then DNA was purified using phenol-chloroform method.

## 15. Animal

A unique, isogenic mouse strain derived from a C57BL/6J (B6) and 129S1/SvImJ background (B6/129) was created and maintained with inbreeding. Pure B6;129-Trp53bp1<sup>tm1Jc</sup>/J were purchased from MacroGen life Science Institute. And B6;129-Trp53bp1<sup>tm1Jc</sup>/J was genotyped use primers like wild type : CTCCAGAGAGAACCCAGCAG;

common: GAACTTCCCTCACACCCATT; mutant reverse : CTAAAGCGCATGCTCCAGAC.

For spermatogenesis study, adult (8 weeks old, 30-35g body weight) 53BP1 WT and 53BP1 KO male mice were used. For glucose-dependent lipogenesis assay, the mice fed a western diet (21%

fat, 50% carbohydrate, and 20% protein) from Research Diet (New Brunswick, NJ) or a fat-free, carbohydrate-rich diet (60.2% sucrose and 20% casein) from ICN (Irvine, CA) for 3 months.

All mice were housed in a 12 h light–12 h dark cycle in a 21–23 °C facility and were euthanized at varying time points following initiation of dietary intervention. All procedures were performed according to protocols approved by the Animal Care and Use Committee of ChosunUniversity All experiments were conducted according to the principles and procedures outline

## **16. Analysis of cholesterol and triglyceride**

Collect whole blood in a covered test tube. Centrifuging at 1000-2000 x g for 10 minutes in a refrigerated centrifuge. the supernatant is serum. In Liver sample, 40-50mg of liver tissue were homogenized in 1.5ml of mixture of CHCL<sub>3</sub>-CH<sub>3</sub>OH(2:1, v/v), followed by shaking at room temperature for 2hr. After addition of 0.5ml of 0.1M Nacl, the suspension was centrifuged at

3700rpm for 10min at room temperature. Serum and liver levels of TG and CHO used Kit from ASAN Company.

## **17. Immunohistochemistry**

Testes were dissected out from mice washed twice in PBS and fixed in Bouin's solution (Sigma-Aldrich). Samples were washed in 70% ethanol and dehydrated. After embedding in paraffin, six-micrometer sections were de-waxed with xylene, rehydrated in decreased concentrations of ethanol, and stained with respective antibodies: rabbit anti-acetyl H4 (H4 Ac.)(1:250, Millipore).

## **18. mtDNA Damage repair**

Quantification of mtDNA damage was done by a quantitative PCR (RT-PCR) that amplifies long DNA targets as previously described (33). Briefly, the following primers were used to amplify an 8.9-kb fragment of mtDNA: 5-TCT AAG CCT CCT TAT TCG AGC CGA-3 (sense) and 5-TTT CAT CAT GCG GAG ATG TTG GA-3 (antisense). A 221-bp fragment of mtDNA was also ampli-

fied to normalize to the copy number of the mitochondrial genome present: 5-CCC CAC AAA CCC CAT TAC TAA ACC CA-3 (sense) and 5-TTT CAT CAT GCG GAG ATG TTG GA-3 (anti-sense).

## **19. Immunofluorescence microscopy**

Cells were fixed with 4% paraformaldehyde, permeabilized with 0.5% Nonidet-P40 (Bioshop, Burlington, ON, Canada) for 15 min, washed and then blocked with 5% bovine serum albumin in PBS for 1 h. Primary antibody incubation was carried out overnight at 4 °C.  $\alpha$ -tubulin (1:200; Sigma);  $\gamma$ -tubulin (1:200 Ab FRONTIER). The secondary antibodies 1:200 used were as follows: Alexa Fluor 488 anti-mouse (Molecular Probes; A-11029), and Alexa Fluor 594 anti-rabbit (Molecular Probes, Eugene, OR, USA; A-11034). Cells were visualized with the Olympus Deconvolution fluorescence microscope.

## 20. Fiber assay

For nascent strand degradation analysis, asynchronous cells were pulse-labeled with 500  $\mu$ M IdU for 1hr, washed three times with medium, incubated with 5 mM HU or medium for 8hr. For DNA replication fork restart analysis, cell were synchronized by serum starvation for 24hr, released in presence of serum, and labeled in S phase for 20min with IdU and then for 2hr with CIdU in the presence of 5mM HU. And washed and maintained in HU-containing medium for 16hr. Wash cell with ice cold PBS, and prepare cell lysate as  $7.5 \times 10^5$  cells/ml in PBS. Use 2  $\mu$ l cell lysate drop to cover slide, air-dry for 5min or until the volume of the drop in greatly reduced but not dry, then drop 7  $\mu$ l lysis solution (50mM EDTA, 0.5% SDS, 200mM Tris-HCL (PH7.5)).air-dry, then fixing with methanol : acetic acid = 3:1 for 10min.

For immunostaining, DNA-stretched coverslips were denatured (2.5N HCL for 45 min), neutralized (0.1 M sodium borate and 3 washes with PBS), blocked (5% BSA and 0.5% Tween 20 in PBS for 30 min), incubated with primary antibodies (Anti-IdU/BrdU or both antiIdU/BrdU and anti-CIdU/BrdU for 30 min), washed (1% BSA and 0.1% Tween 20 in PBS, 3 times 5 min each)

and incubated with secondary antibodies (anti-mouse Alexa Fluor 488-conjugated, or both anti-mouse Alexa Fluor 488-conjugated and anti-rat Alexa Fluor 594-conjugated for 1 h). Washed slides were mounted in prolong gold anti-fade reagent (Life Technologies) and images were sequentially acquired (for double-label) with LAS AF software using TCS SP5 confocal microscope (Leica). A 63×/1.4 oil immersion objective was used. Images were captured at room temperature.  $n \geq 300$  fiber tracts scored for each dataset. The DNA tract lengths were measured using Zen2011 and the pixel length values were converted into micrometers using the scale bars created by the microscope. Statistical analysis was done using Excel program.

## RESULT

### 1. 53BP1 interacts with ACL

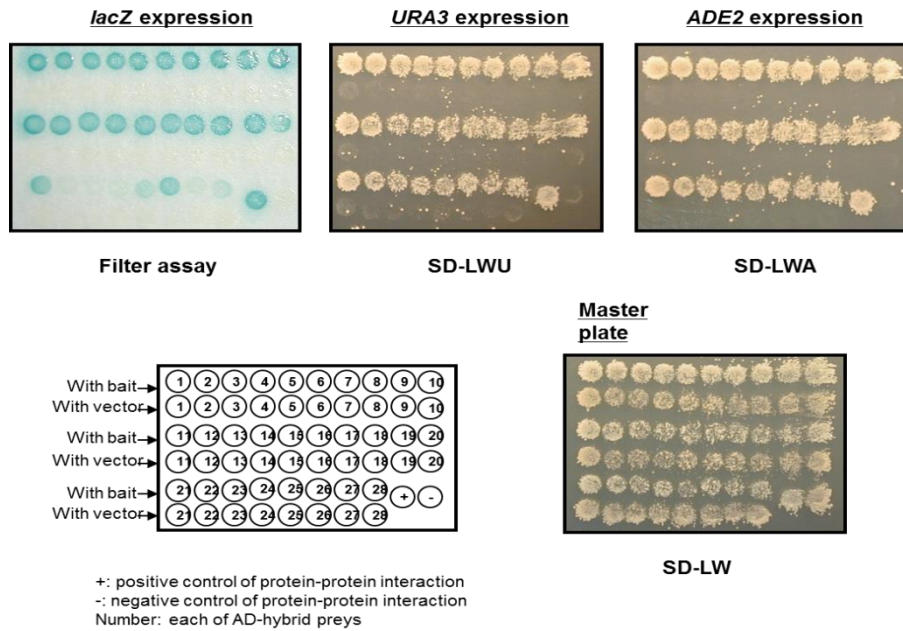
#### i. ACL; Novel binding protein of 53BP1

Yeast two-hybrid screening represents a sensitive *in vivo* method for the identification and analysis of protein-protein interactions. The principle is based on the ability of a separate DNA-binding domain (DNA-BD) and activation domain (AD) to reconstitute a functional transactivator when brought into proximity.

In order to explore the unknown 53BP1 interacting protein yeast two-hybrid screening for the N-terminal fragment (a.a 1-699) human 53BP1 as bait was carried out. Out of the  $2 \times 10^6$  transformants that were screened, 28 independent positive clones were isolated (Figure 3A).

Through this screen we identified novel putative 53BP1-associated proteins including ACL (NM\_001096), NCAPH (NM\_015341), H2AX (NM\_006118), Sertad1 (NM\_013376), TAF1 (NM\_138923), NQO2 (NM\_000904) and DNAJB6 (NM\_005494). Among these, ACL was most relevant because many clones were presented (Figure 3B).

A



B

AD-Hybrid-1-6 : ACLY transcript1 (NM\_001096)  
 AD-Hybrid-5-10 : ACLY transcript 2 (NM\_198830)  
 AD-Hybrid-11-18 : NCAPH (NM\_015341)  
 AD-Hybrid-19-22 : H2AX (NM\_006118)  
 AD-Hybrid-23-25 : SERTAD1 (NM\_013376)  
 AD-Hybrid-26 : TAF1 (NM\_138923)  
 AD-Hybrid-27 : NQO2 (NM\_000904)  
 AD-Hybrid-28 : DNAJB6 (NM\_005494)

**Figure 3. 53BP1 as a ACL-associated protein.** (A) Protein interaction study by Yeast two-hybridization assay. (B) 53BP1-associated proteins.

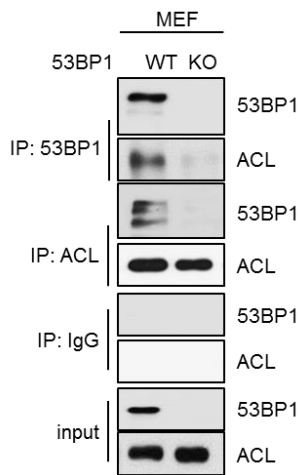
## ii. Binding of 53BP1 and ACL in both of vitro and vivo.

To con showed that 53BP1 mainly localized in nucleus, but ACL localized in the nucleus as well as the cytoplasm at MEF and 293T cells (Figure 4C - a and b). Interestingly, there was a stronger associated between 53BP1 and ACL in cytoplasm (Figure 4D-a). We then showed that this interaction takes place in vivo by demonstrating that HA-tagged 53BP1 co-immunoprecipitated with GFP-tagged ACL in HEK 293T cells (Figure 4D-b). To confirm this finding, we used GST-pull down to confirmed the results of vivo. We purified GST fusion protein of 53BP1 N-terminal fragment (a.a 1-699), and used recombinant human protein ACL from Sino Biological Inc. we found that recombinant human ACL protein interacted with N-terminal domain of 53BP1 (a.a 1-699) but not GST alone, suggesting that ACL directly binds to this region of 53BP1 in vitro (Figure 4E).firm that 53BP1 and ACL interact with each other under physiological conditions, we used co-immunoprecipitation assays followed by western blotting to protein-protein interactions. Immortalized MEF 53BP1 wild type (WT) and 53BP1 knockout type (KO) cells were lysed and performed co-immunoprecipitation, using antibodies against 53BP1 and ACL. As shown in Figure 4A, endog-

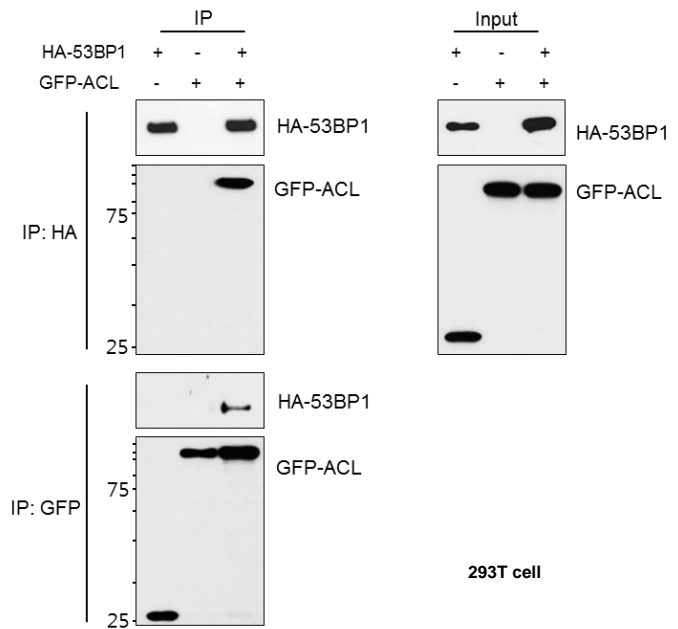
enous 53BP1 and ACL co-immunoprecipitated reciprocally, but not with the immunoglobulin G (IgG). Our endogenous binding results were further confirmed by exogenous co-Immunoprecipitation using full length HA-53BP1 and GFP-ACL. HEK 293T were transfected with full-length 53BP1 tagged with HA and GFP tagged ACL. Co-Immunoprecipitation assay were performed by using an anti-HA antibody and immunoblotting was done with anti-GFP antibody, results similar to endogenous co-Immunoprecipitation (Figure 4B).

ACL localizes to both the cytoplasm and nucleus [4] and 53BP1 also localizes to both cytoplasm and nucleus. However, although the nuclear functions of 53BP1 in the DDR and in the choice of DNA repair pathway are well established, the role of 53BP1 in cytosol remains unknown. We

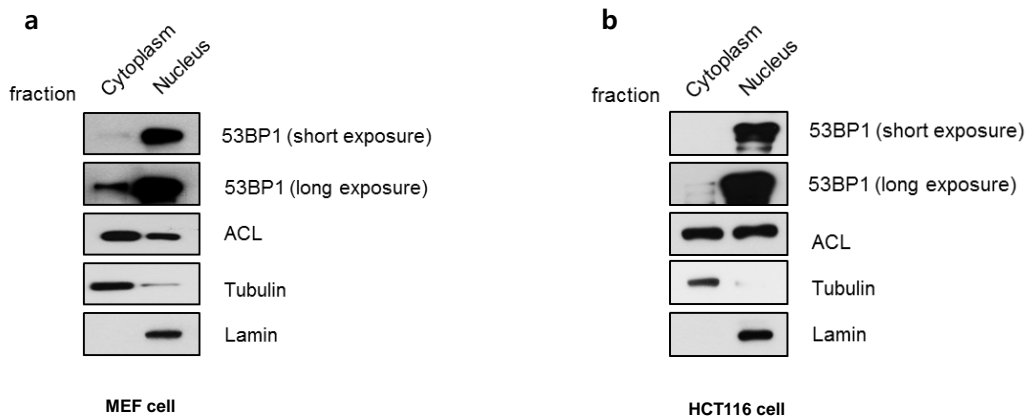
**A**



**B**

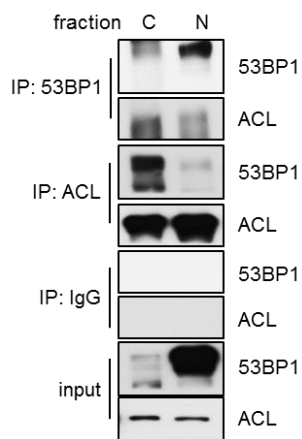


**C**



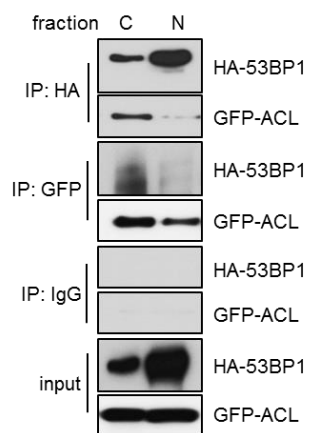
**D**

**a**



MEF cell

**b**



293T cell

**E**

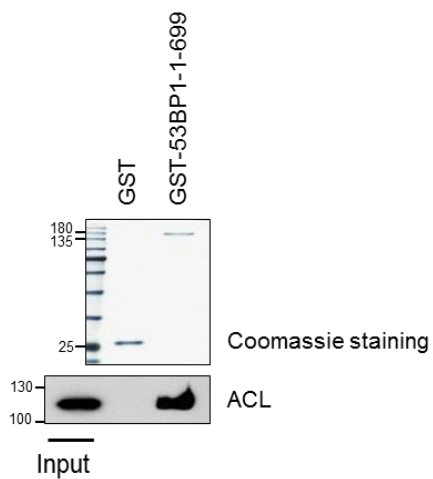


**Figure 4. Binding of 53BP1 and ACL in both of vitro and vivo**

(A) Endogenous IP used immortalities MEF cell and an anti-53BP1 or anti-ACL antibody was used.

(B) HA-53BP1 interacts with GFP-ACL (exogenous). HEK293T cells were transfected with full-

length HA-53BP1 and GFP-ACL expression vectors. Proteins were immunoprecipitated from the

lysates using an anti-HA or GFP antibody. (C) Mouse cell line immortalities MEF (a) and human

cell line HCT116 (b) fraction to check localization of 53BP1 and ACL. (D) Fraction endogenous-

IP in immortalities MEF (a) and fraction exogenous-IP in human cell line HEK293T (b). (E) In

vitro GST-full down.

### **iii. The N-terminal region of 53BP1 mediates the interaction with ACL**

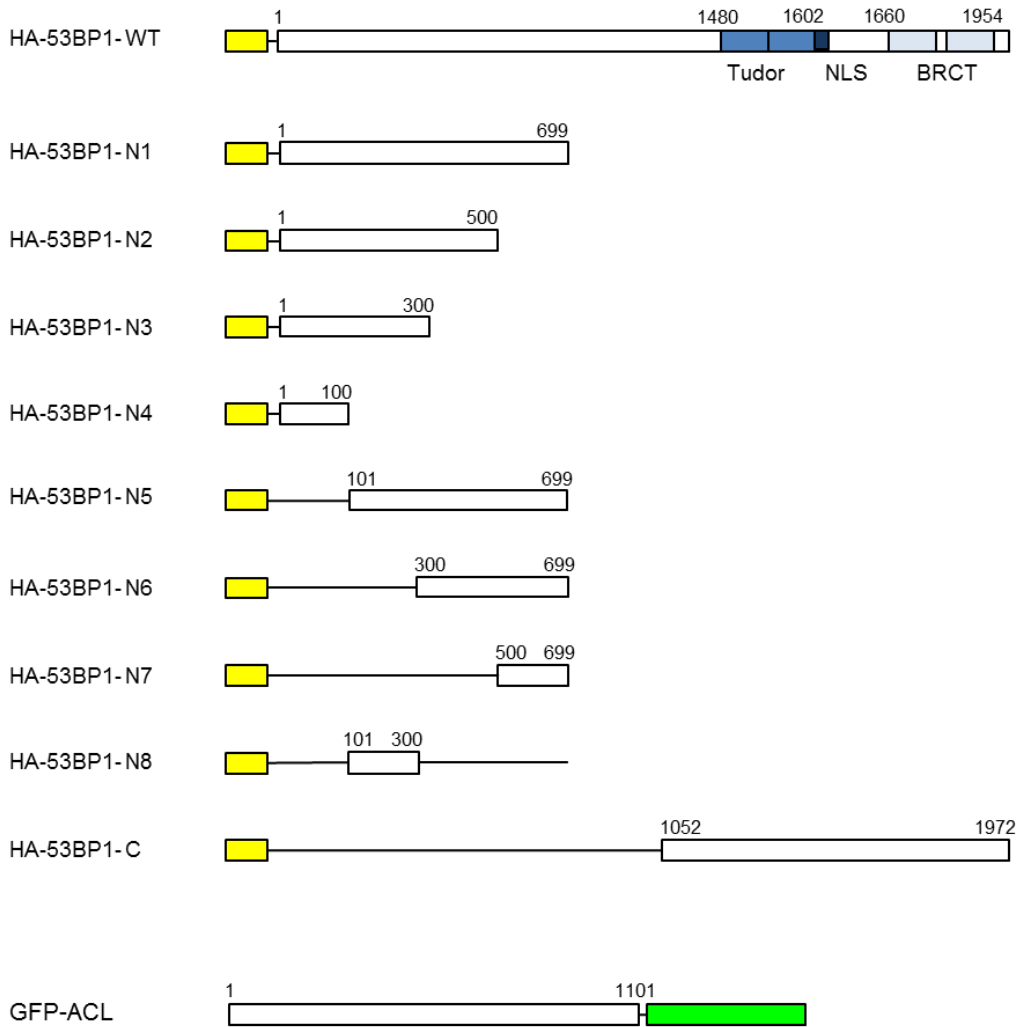
To identify which regions of 53BP1 interact with ACL, we subjected HA-tagged 53BP1, including wild type and a series of mutants containing internal deletion. To co-immunoprecipitation experiments using GFP-tagged ACL (Figure 5A).

Yeast two-hybrid screening showed that ACL protein is interacting strongly at N-Terminal (a.a 1-699) of 53BP1, to confirm this, we used two 53BP1 fragments N-Terminal (a.a 1-699) and C-Terminal (a.a 1052-1838). 293T cells were transfected with full length GFP-ACL and HA-53BP1 N-Terminal N4 or C-Terminal C2. The result showed that GFP-ACL specific binding with HA-53BP1 N-Terminal but not C-Terminal (Figure 5B).

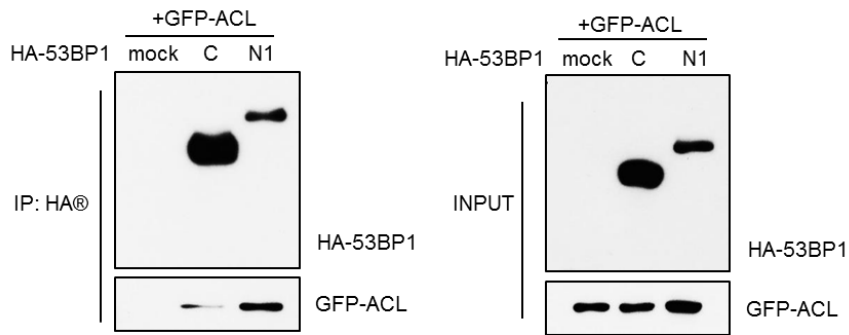
To identify ACL binding domain with 53BP1, we used eight 53BP1 fragments consisting of residues N1-N8 (Figure 5A). N1 (a.a 1-699), N2 (a.a 1-500), N3 (a.a 1-300), N4 (a.a 1-100), N5 (a.a 101-699), N6 (a.a 301-699), N7 (a.a 501-699), N8 (a.a 101-300). HEK 293T cells were co-transfected with 53BP1 constructs N1-N8 and full length GFP-ACL. The cells were lysed and co-immunoprecipitated by using an anti-HA antibody and then immunoblotting was done with anti-

GFP antibody. Co-immunoprecipitation results showed us 53BP1 construct N8 (a.a 101-300) did not shown any band. These results indicate us binding site of ACL is region N4 (a.a 1-100) and N6 (a.a 301-699) (Figure 5C).

A

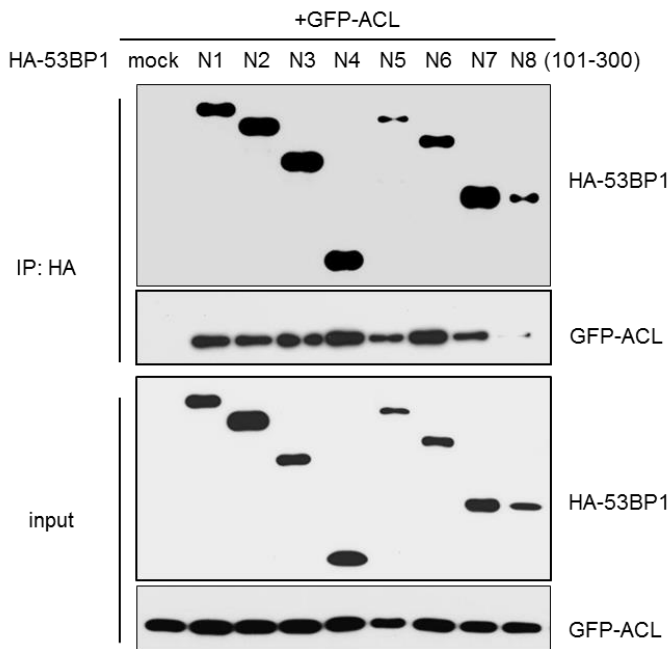


**B**



293T cell

**C**



293T cell

## Figure 5. Identification of a ACL Binding site/domain in 53BP1

(A) Schematic representation of 53BP1 full length and other constructs. (B) GFP-ACL interacts with N-terminor of HA-53BP1 but not C-terminor, used HEK293T cell. (C) Co-Immunoprecipitation of GFP-ACL and 53BP1 constructs N1-N8 used HEK 293T cell. Proteins were immunoprecipitated from the lysates using an anti-HA® antibody. Immunoprecipitates were then subjected to western-blot analysis using antibodies specify for GFP-ACL antibody. The second or third western blotting contains 20% input for GFP-ACL and HA-53BP1 constructs N1-N8 and control HA vector.

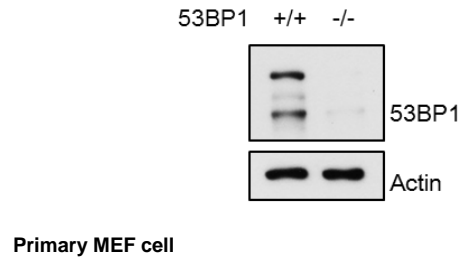
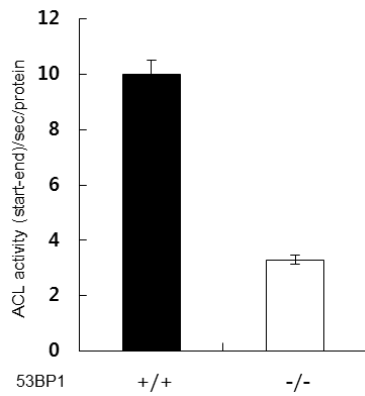
## 2. 53BP1 regulates ACL activity

To examine the potential role of 53BP1 through binding of ACL, we asked whether 53BP1 induced ACL activity. We chose mouse cell line MEF and two human cell lines, HeLa and 293T. MEF used 53BP1 WT type and 53BP1 KO type, and for human cell lines, we transfected with control or 53BP1 siRNA. The ACL activity in cell extracts was measured. In 53BP1 deficient mouse and human cells and knockdown cells resulted about 20% decrease of ACL activity than control cell line. The effect of 53BP1 knockdown was weaker than ACL knockdown, but it was still significant (Figure 6A). Next, to examine this further, 293T cells were co-transfected with GFP-ACL full length plasmid and/or HA-53BP1 full length plasmid, and then measured ACL activity. As shown in Figure 6B the ratio of ACL activity was increased much more in co-transfected with 53BP1 and ACL plasmid sample than only transfected ACL plasmid sample. This suggests that 53BP1 may affect the ACL activity by interact with ACL protein (Figure 6B). In Figure 5B we showed that GFP-ACL specific binding with HA-53BP1 N-Terminal but not C-Terminal domain. To determine whether N-terminal domain of 53BP1 controls ACL activity, 293T cells co-transfected with full

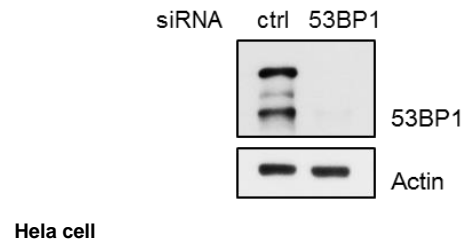
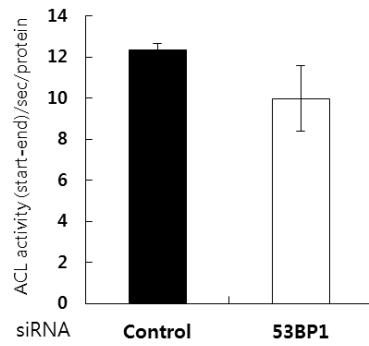
length GFP-ACL and HA-53BP1 N-terminal plasmid or C-terminal plasmid, respectively. The ratio of ACL activity was increased at 53BP1 N-terminal plasmid co-transfected sample (Figure 6C), this result indicate that ACL activity regulated by 53BP1 perhaps through binding with N-terminal domain but not C-terminal domain of 53BP1.

**A**

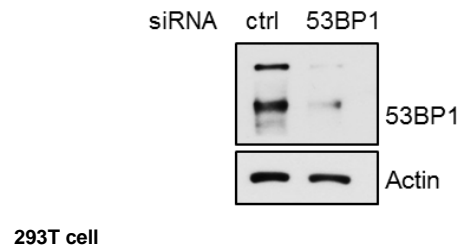
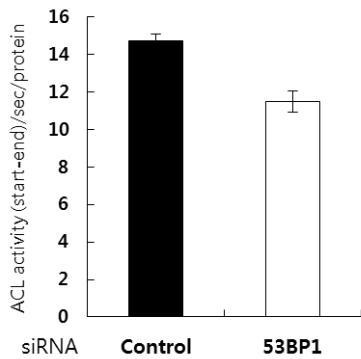
**a**



**b**



**c**



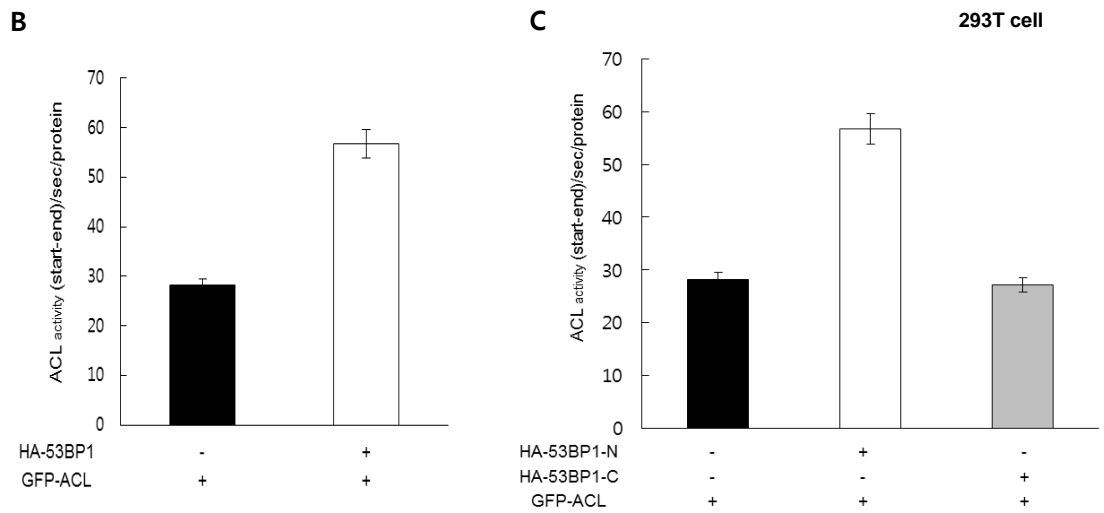


**Figure 6. 53BP1 regulates ACL activity**

(A) ACL activity in 53BP1 knockout or knockdown cell lines. (a) primary MEF (b) Hela (c) HEK 293T. (B) HEK 293T co-transfection with GFP-ACL full plasmid and HA-vector or HA-53BP1 full plasmid. (C) HEK 293T co-transfection with GFP-ACL full plasmid and HA-53BP1-N1 or HA-53BP1-C

### 3. Mice deficient in 53BP1 exhibit decreased body weight and fat formation

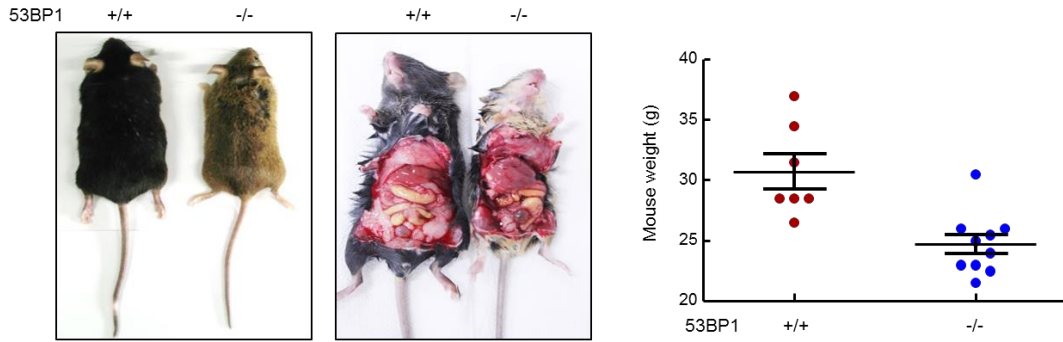
A key enzyme linking lipid biosynthesis is ATP citrate lyase. In Figure 4D , we showed that 53BP1 binds with ACL especially in cytoplasm, and regulates the activity of ACL. So, we suspected that 53BP1 knockout mice might exhibit reduced body weight decreased fat formation. As shown in Table 1 and Figure 7A, the whole body weight was decreased in 53BP1 KO mice compared WT mice. In addition, there have two types of fat in humans and other mammals –one type is brown fat, and the other type is known as white or yellow fat. Brown fat is often referred to as the “good” fat, since it helps us burn, not store, calories. White fat has many purposes. It provides the largest energy reserve in the body. Also it is the main reason of obesity. Our data showed that white fat and brown fat lower in 53BP1 KO mice (Table. 1 and Figure 7B). However, the levels of cholesterol and triglyceride in Liver tissue and serum of the 53BP1 WT and KO mice were similar (Figure 7C). Taken together, our data showed that 53BP1 KO mice have reduced body weight and lower fat formation as a result of a decreased capacity for lipid synthesis. However, the levels of cholesterol and TG were no different in 53BP1 WT and KO mice.

ATP-citrate lyase (ACL) is a crucial lipogenic enzyme that regulates the flow of glucose carbons to cytosolic acetyl-coenzyme A (CoA) by catalyzing an ATP-consuming reaction to generate acetyl-CoA from citrate, thereby linking cellular glucose catabolism and *de novo* lipid synthesis [24],[25]. Acetyl-CoA is further converted to malonyl-CoA by acetyl-CoA carboxylase (ACC), the rate-limiting step in *de novo* fatty acid synthesis. Fatty acids are subsequently synthesized from malonyl-CoA by fatty acid synthase (FAS), long-chain elongase (ELOVL6), and stearoyl-CoA desaturase 1 (SCD1); and formation of triglycerides is catalyzed by another series of enzyme, such as glycerol-3-phosphate acyltransferase (GPAT) and diacylglycerol acyltransferase (DGAT) [23]. To identify mRNA expression levels of genes related to fatty acid oxidation/transport between 53BP1 WT and KO mice, Realtime PCR and western blot sample from livers were performed. Although, there have no significant difference in mRNA expression of ELOVL6, SCD1, GPAT, DGAT (data not show). The protein expression of FAS and ACC were decreased in 53BP1 KO mice sample (Figure 7D).

**Table. 1 Physiologic Data of 53BP1 Wild and Knockout Type Mice**

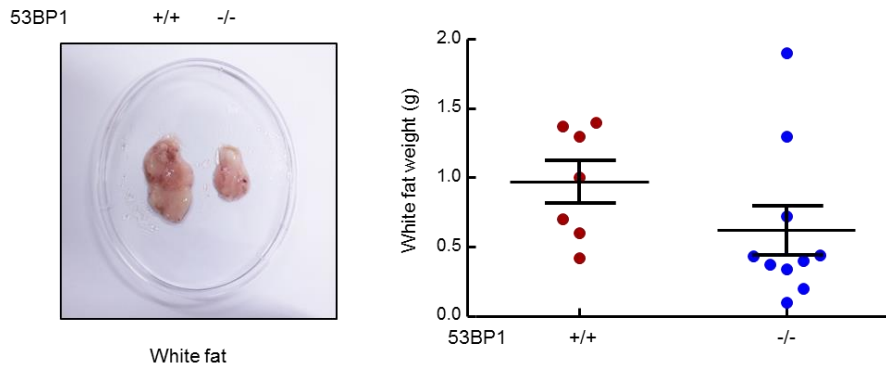
	<b>53BP1-WT-western (n=7)</b>	<b>53BP1-KO-western (n=11)</b>
<b>Heart</b>	0.23±0.13	0.212±0.1
<b>Brain</b>	0.53±0.11	0.368±0.12
<b>Spleen</b>	0.15±0.08	0.133±0.12
<b>Lung</b>	0.5±0.15	0.264±0.13
<b>Liver</b>	1.96±0.57	1.222±0.23
<b>Muscle</b>	0.83±0.38	0.804±0.3
<b>Kidney</b>	0.56±0.11	0.434±0.1
<b>Testie</b>	0.33±0.14	0.244±0.08
<b>Pancreas</b>	0.36±0.13	0.227±0.09
<b>white Fat</b>	0.97±0.4	0.62±0.56
<b>brown Fat</b>	0.4±0.16	0.19±0.1
<b>weight</b>	30.7±3.8	24.7±2.6

**A**

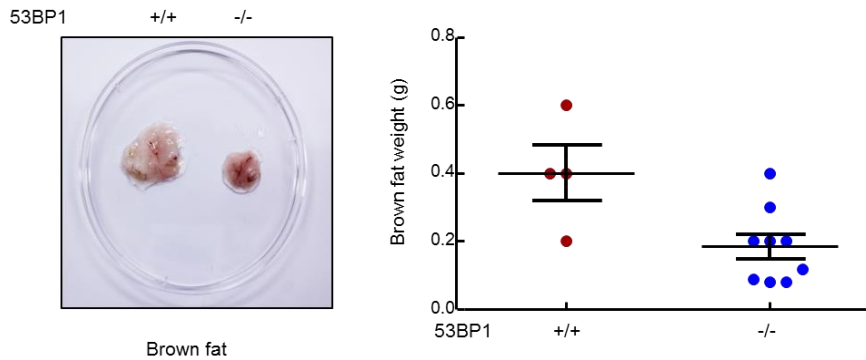


**B**

**a**



**b**



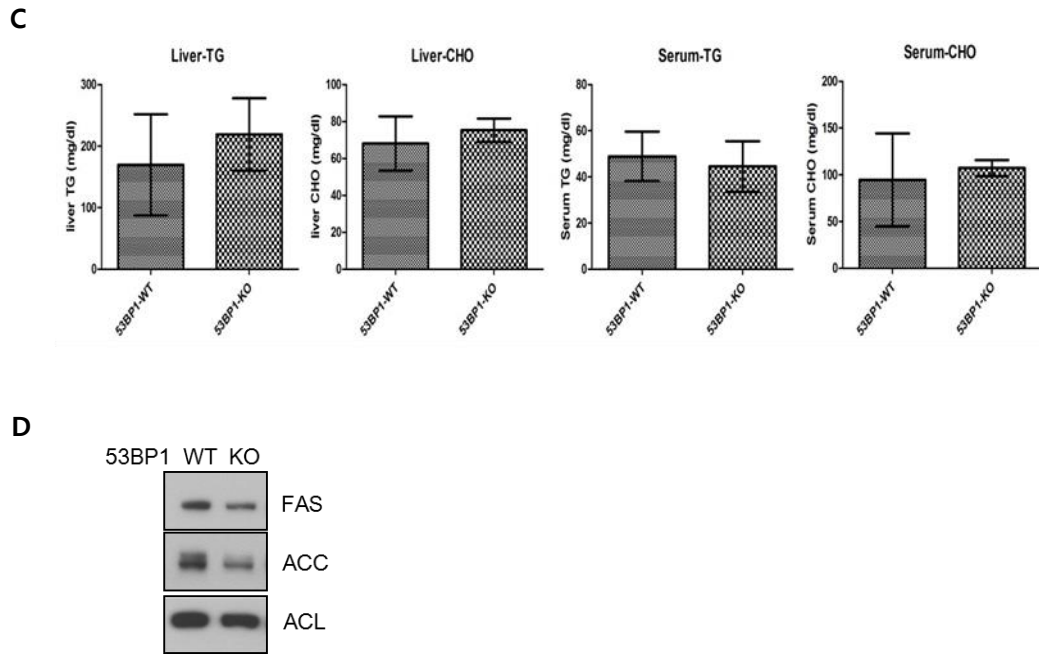


### Figure 7. Deficiency in 53BP1 Results in Mice Physiologic Data

All data are from 17-week-old male B57BL/6J 53BP1 WT or KO type mice (n=7 per group).

western diet or high glucose diet fed for 3-monthes.  $P < 0.05$ .

(A) Western diet group 53BP1 WT type (left) and KO type (right) (B) white fat (a) and brown fat

(b) from 53BP1 WT type and KO type mice. (C) Western diet group analysis liver tissue or se-

rum CHO and TG. (D) Western bolt samples from 53BP1 WT or KO mice liver tissue (n=3).

## 4. 53BP1 regulates histone acetylation

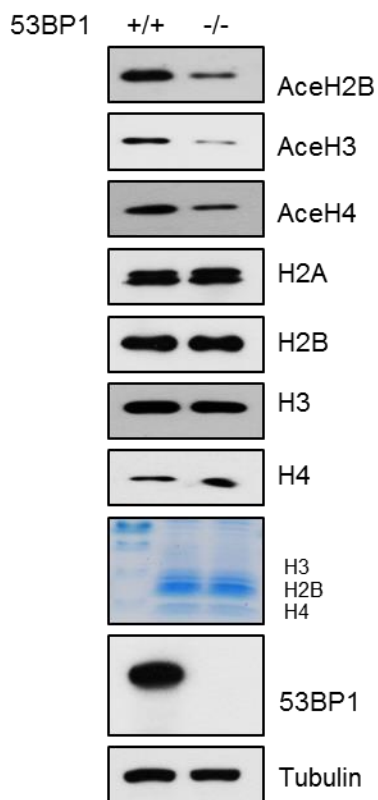
### i. Deletion of 53BP1 leads to decreased Histone acetylation

Wellen *et al.* reported that ACL activity is required to link growth factor-induced increase in nutrient metabolism to the regulation of histone acetylation. In Figure 6, we showed that ACL activity regulated by 53BP1, to investigate whether 53BP1 is important for the maintenance of histone acetylation in mammalian cells, we analyzed histone acetylation in 53BP1 deficient primary MEF and human cell lines. In 53BP1 KO MEF and 53BP1 knockdown HCT116 cells, global histone acetylation was decreased, these results agreement with silencing of ACL as Wellen et al. (Figure 8A-a). we also check whether 53BP1 have an influence on specific histone acetylation at K5 of H2A, K5 of H2B, K9, K14, K18, K27, K56 of H3 and K5, K8, K12, K16 of H4. Acetylation of histones at specific lysine residue was reduced by more than 50% in cells, as compared to that of control cells (Figure 8A-b). Similar results were obtained in immortalized MEF, and other human cells, such as A549 and 293T cells (Figure 8A c-e). Thus, 53BP1 was required for histone acetylation.

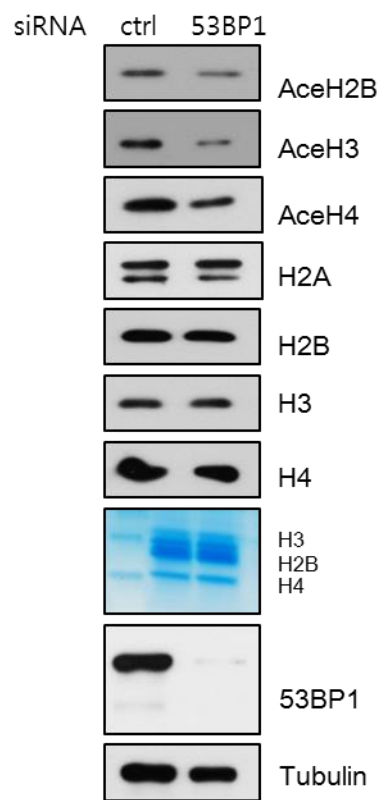
Notably, depletion of both 53BP1 and ACL did further decrease histone acetylation from what was observed with 53BP1 depletion alone (Figure 8B a,b), indicating that 53BP1 has ACL-mediated pathway and other additional pathway. Introduction of 53BP1 construct into MEF cells knockout of 53BP1 restored histone acetylation, and we also confirmed the result with human cell line 293T (Figure 8C a,b).

A

a

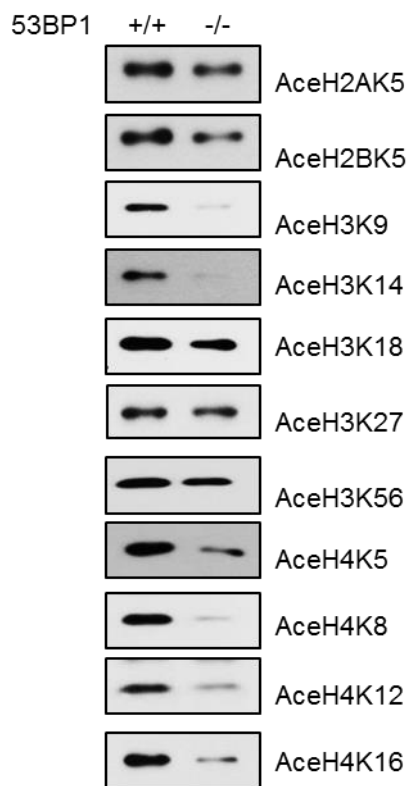


Primary MEF cell

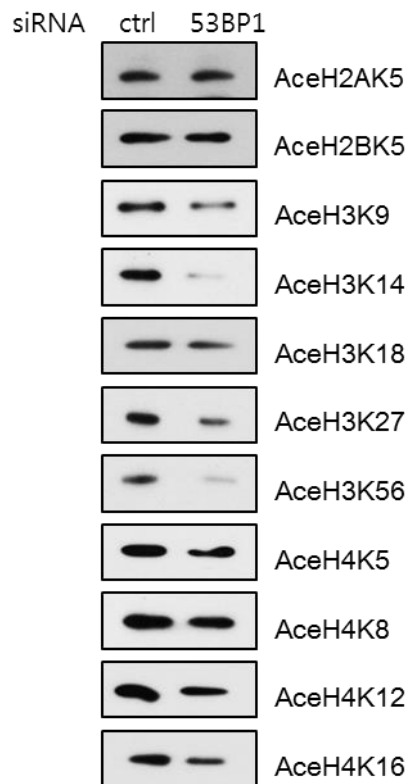


HCT116 cell

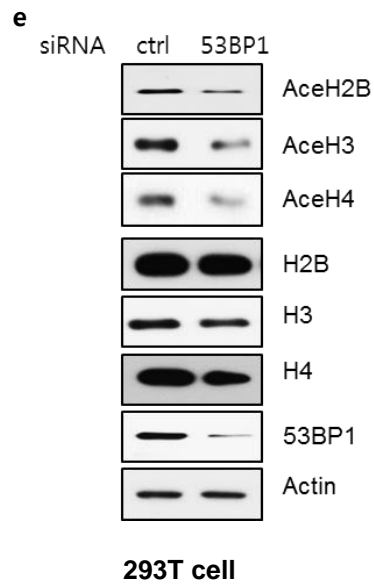
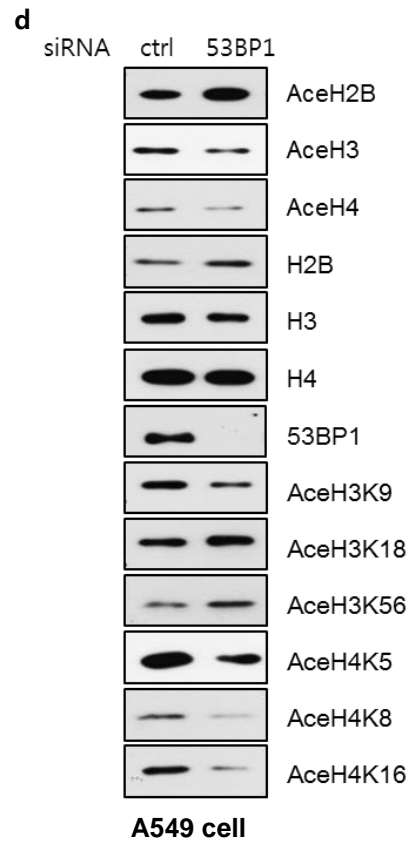
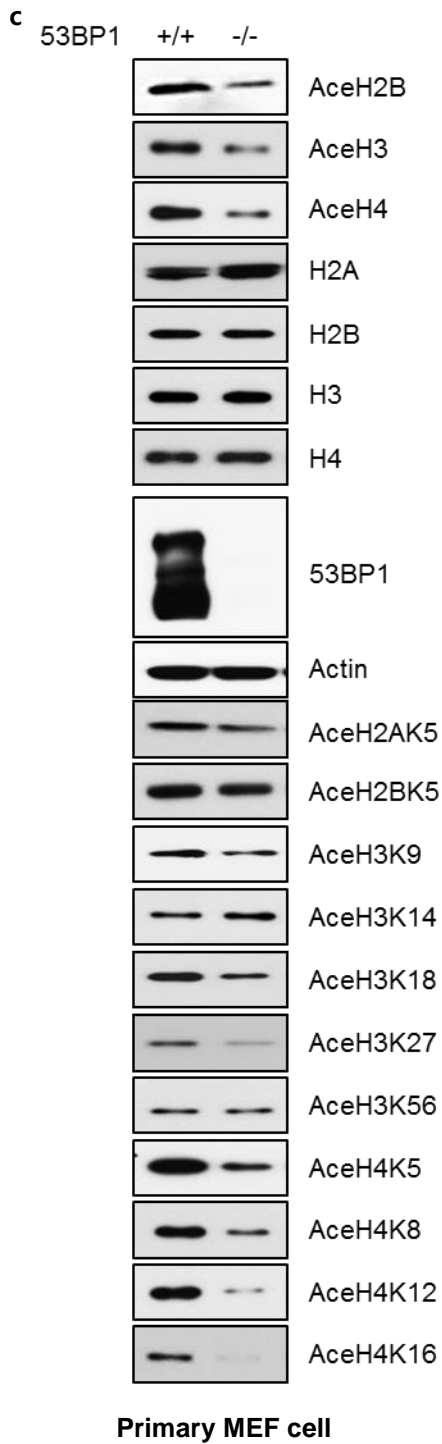
**b**



**Primary MEF cell**

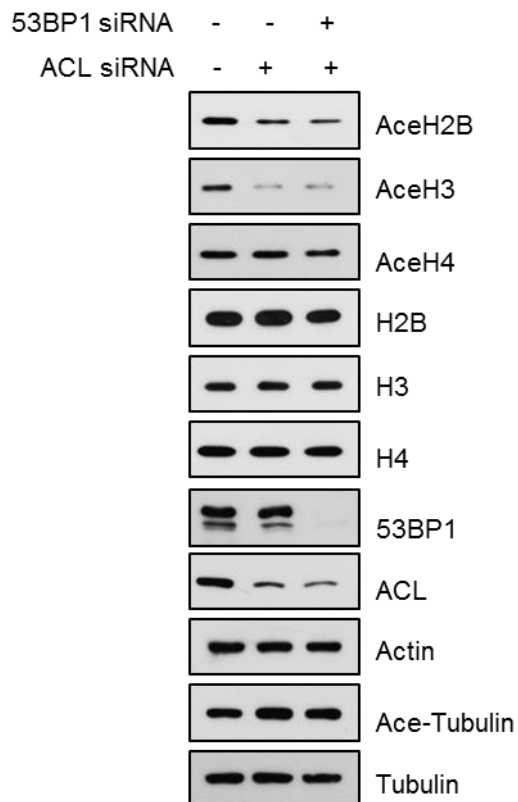


**HCT116 cell**



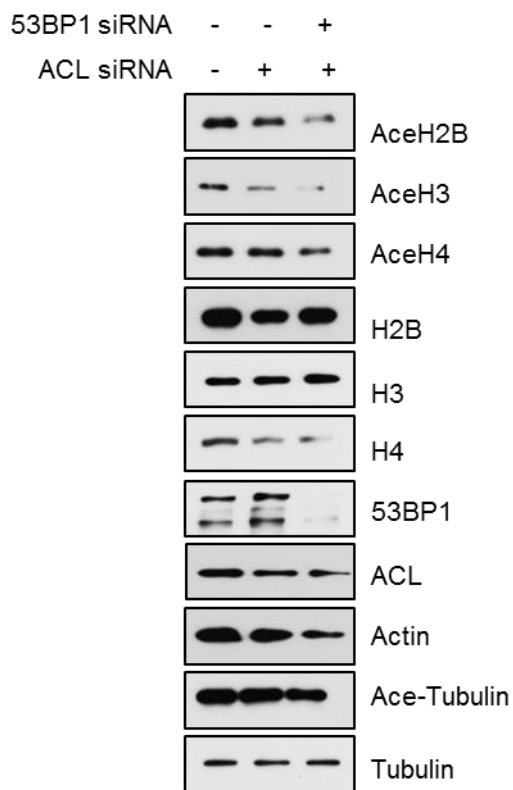
**B**

**a**



**Primary MEF cell**

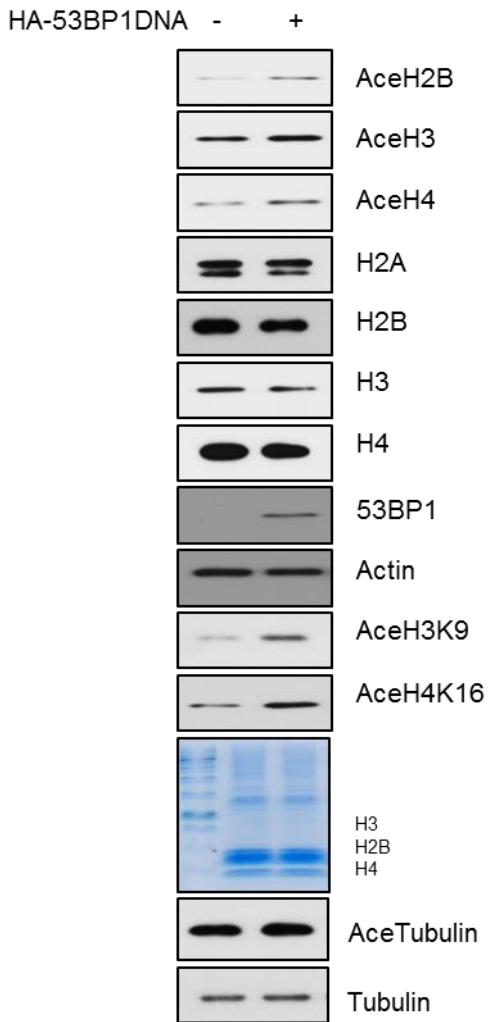
**b**



**HCT116 cell**

**c**

**a**



**Primary MEF cell**

**b**

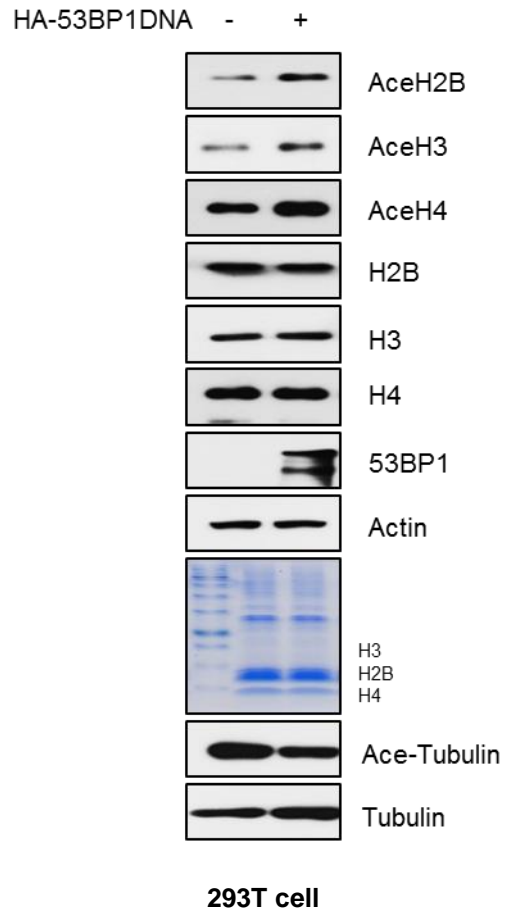
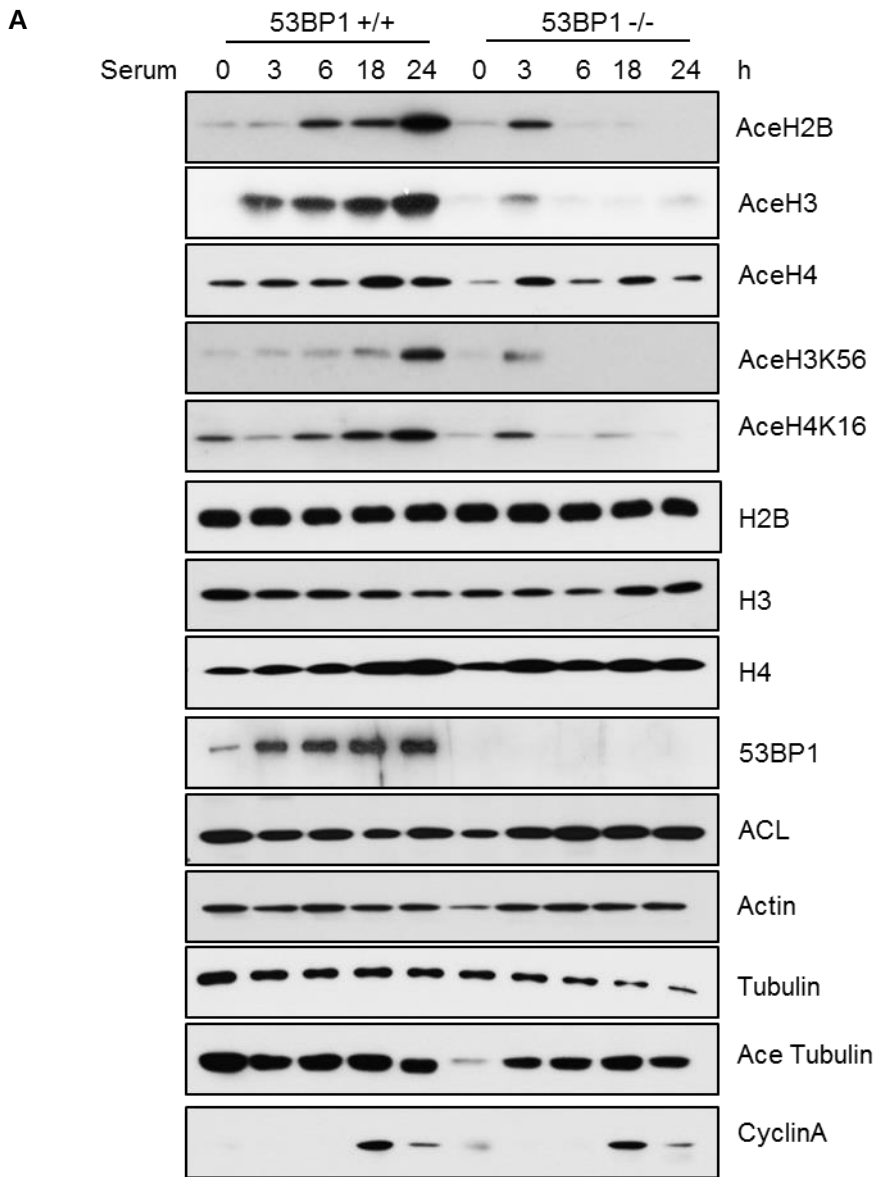


**Figure 8. 53BP1 is important for the maintenance of histone acetylation**

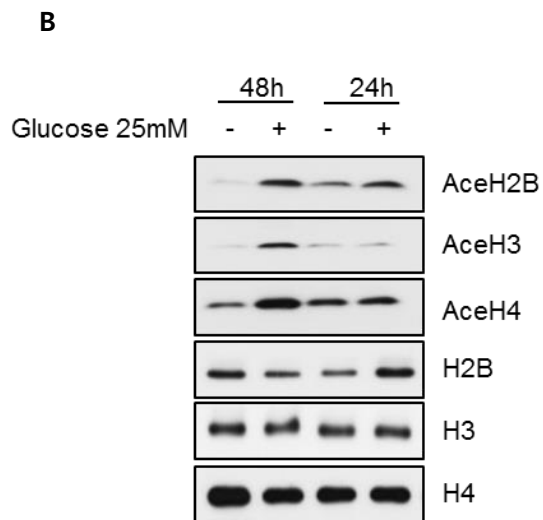
(A) Western blot analysis of total and acid extracts from 53BP1 knockout or knockdown cell. (a) global histone acetylation used primary MEF cell and HCT116 cell, (b) specific histone acetylation used primary MEF and HCT116, (c)-(e) confirmed the global histone acetylation and specific histone acetylation used Immortal MEF cell, A549 cell and HEK 293T. (B) Cells were transfected with control and 53BP1 siRNA as indicated for 48hours. Western blot analysis of total and acid extracts from 53BP1 knockdown cells use (a) primary MEF 53BP1 WT type cell and (b) HCT116 cell. (C) (a) immortal MEF 53BP1 knockout cell and (b) used human cell line HEK 293T. transfected with HA-53BP1 full plasmid, after 48hours harvest samples.

**ii. 53BP1 regulates histone acetylation in the response of serum stimulation and glucose condition**

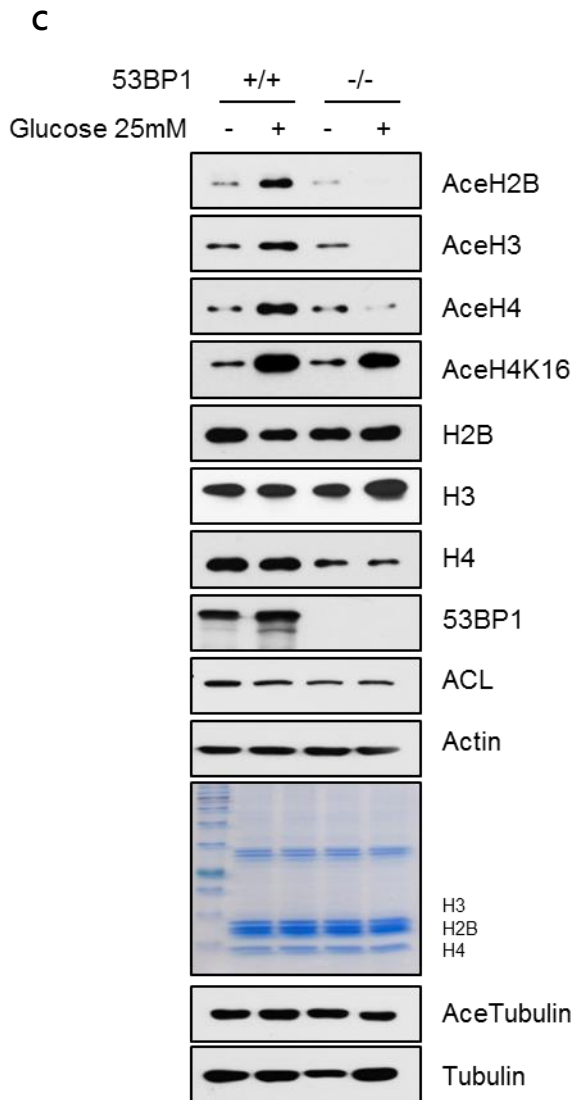
Acetylation of histone is regulated in a cell cycle-dependent manner and can contribute to normal cell cycle progression [26]. We sought to determine whether 53BP1 related with histone acetylation at this condition, we assessed the ability of histone acetylation through cell phase. In 53BP1 WT type cells, histone acetylation increased after serum stimulation, and knockout of 53BP1 inhibited this response. However, levels of acetylated tubulin were unaffected by 53BP1 suppression (Figure 9A). To assess whether histone acetylation by 53BP1 also as ACL, associates with glucose availability. Indeed, serum-induced changes in histone acetylation were dependent on glucose and failed to occur in the absence of 53BP1 (Figure 9B and C).



Primary MEF cell



Primary 53BP1 WT type MEF cell



Primary MEF cell

**Figure 9. 53BP1 regulates histone acetylation in cell cycle and glucose-dependent**

(A) Primary MEF 53BP1 WT and KO cells were used, synchronized by serum deprivation overnight followed by serum stimulation. Cells were harvest at time points (every 3h), after readdition of serum to the culture. (B) western blot analysis of total protein extracts from primary MEF WT cells at indicated times following serum re-introduction in the presence (25mM) or absence (0mM) of glucose. (C) Western blot analysis of total protein and acid extracts from primary MEF WT and KO cells after cultured for 48h in the presence or absence of glucose as described in materials and methods.

### iii. 53BP1 regulates histone acetylation during adipocyte differentiation

Histone acetylation increases have also been observed during differentiation of murine 3T3-L1 preadipocytes into adipocytes [27]. Wellen *et al.* showed that during adipocyte differentiation, global histone acetylation is determined by glucose availability through an ACL-dependent pathway. To establish the functional involvement of 53BP1 in histone acetylation of differentiating 3T3-L1 cell, we analyzed global histone acetylation after siRNA-mediated silencing of 53BP1, ACL, or both. PPAR  $\gamma$  and C/EBP  $\beta$  initiate positive feedback to induce their own expression and also activate a large number of downstream target genes whose expression determines the adipocyte. As ACL, silencing of 53BP1 also reduced histone acetylation in adipocytes (Figure 10A). To examine whether 53BP1 participates in the PPAR  $\gamma$ -dependent adipogenesis, preadipocyte, 3T3-L1 cells were subjected to the adipocyte differentiation. Cells were fixed and Oil Red O lipid staining was performed 5 days after induction of preadipocyte differentiation. Strikingly, in 53BP1-deficient 3T3-L1 cells, the differentiation was apparently inhibited. reflecting by fewer cells containing fat droplets (Figure 10B). Consistently, protein expression of the adipocyte marker genes,

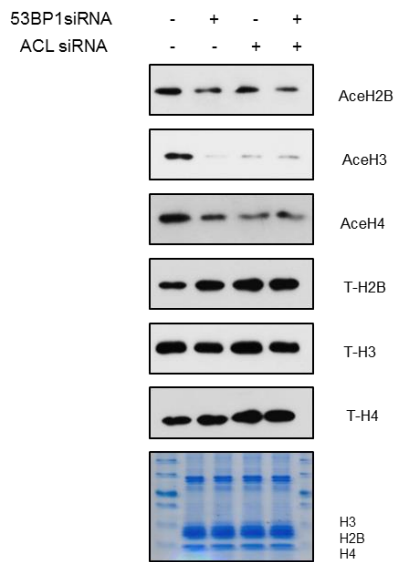
C/EBP  $\alpha$ , PPAR  $\gamma$  and carbohydrate metabolism genes, GLUT4 and PFKI was much lower in 53BP1-defected 3T3-L1 cells at days 4 compared with that in 3T3-L1-control cells (Figure 10C).

Silencing of ACL reduced histone acetylation and lipid accumulation can be partially rescued by acetate (4). So in Figure 10D, 3T3-L1-control and 53BP1-defected 3T3-L1 cells cell extracts from 0 and 4 days after induction of differentiation in the presence of 0, 1, 5 or 10 mM sodium acetate were analyzed by western blot using antibodies of acetyl-histones. Silencing of 53BP1 reduced histone acetylation and could be rescued by acetate. Similarly, in 53BP1 deletion cells reduced lipid accumulation and gene expression could be also partially reused by acetate also (Figure 10E and F).

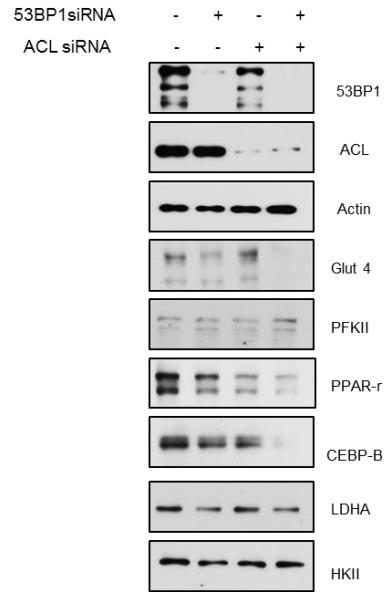
Regulation of histone acetylation and glucose metabolism genes expression by ACL dependent on various concentration of glucose during differentiation, so we next investigated whether the regulation of histone acetylation and gene expression by 53BP1 also dependent on glucose concentration. Standard medium for adipocyte differentiation contains 25mM glucose. In 1mM and 4mM glucose media samples, global histone acetylation was decreased, glucose metabolism genes ex-

pression also decreased in 53BP1-defected 3T3-L1 cells sample, ACL-defected 3T3-L1 cells used as a positive control. Taken together, These results showed that 53BP1 downregulated histone acetylation and gene expression during differentiation of preadipocyte 3T3-L1.

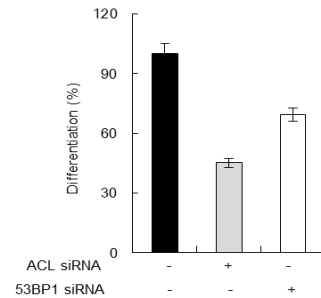
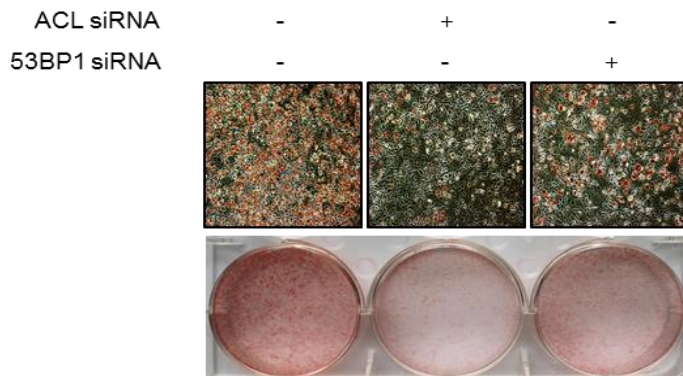
**A**



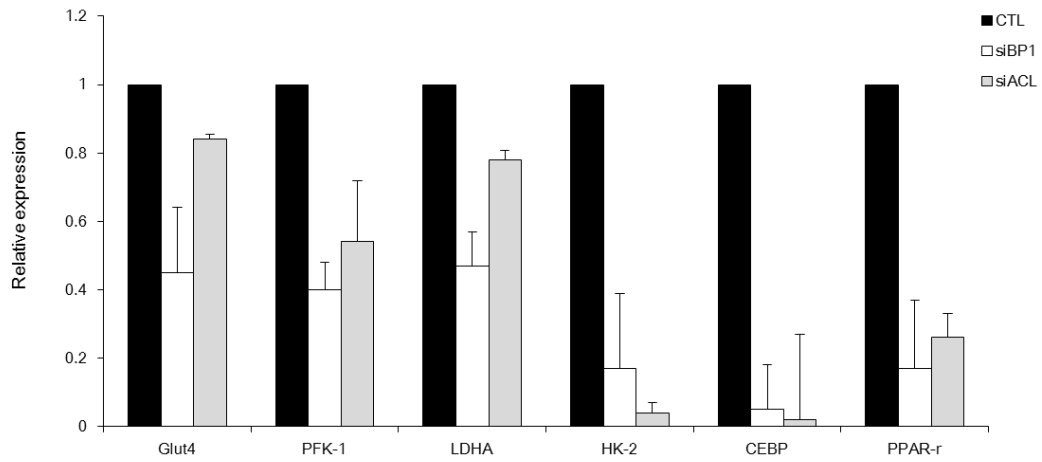
**C**



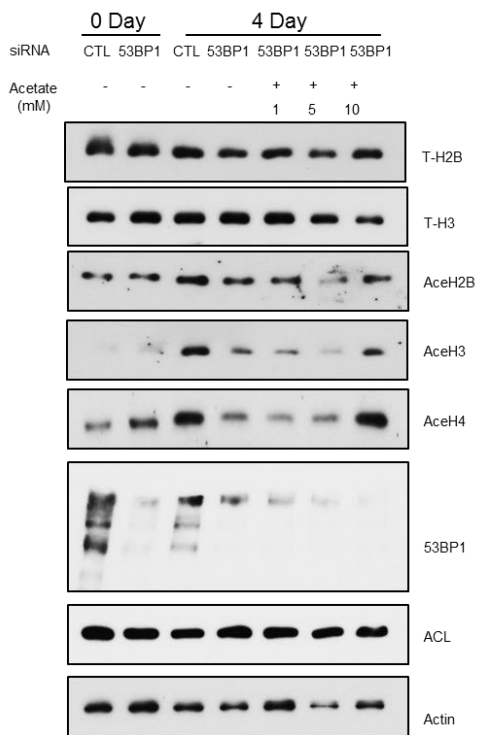
**B**



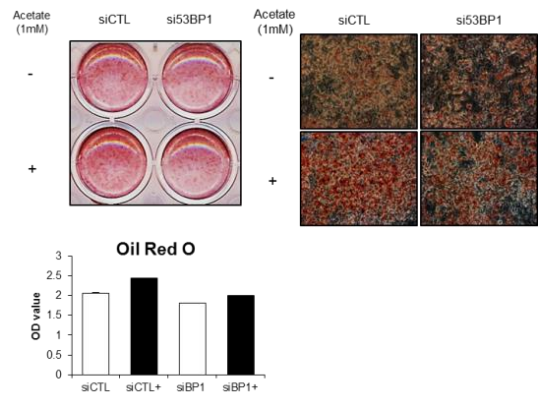
D



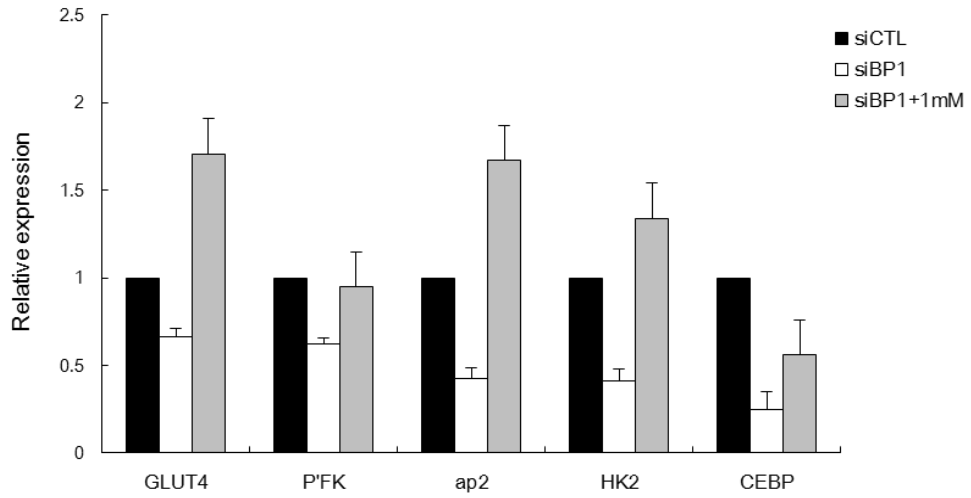
E



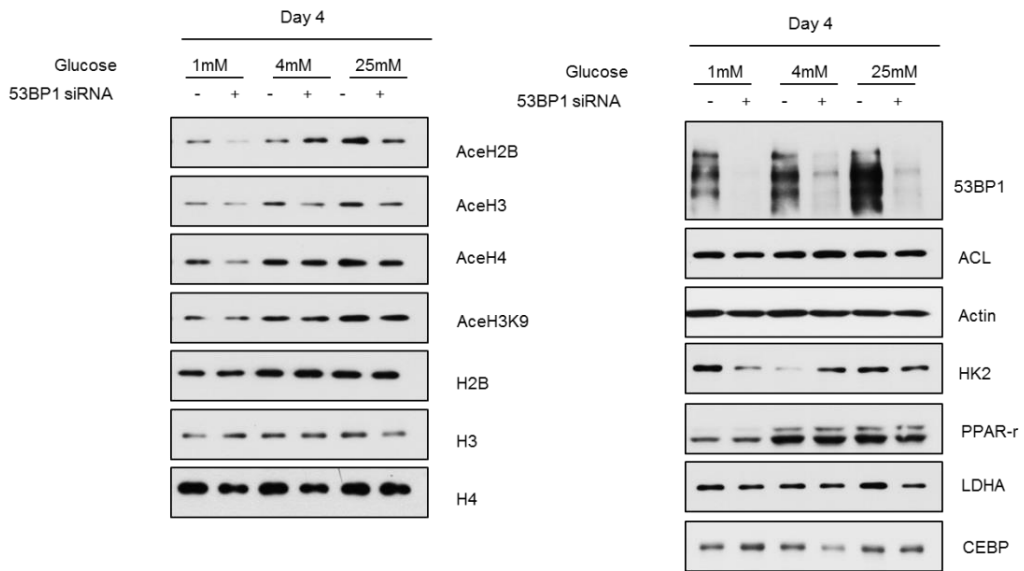
F



G



H



I

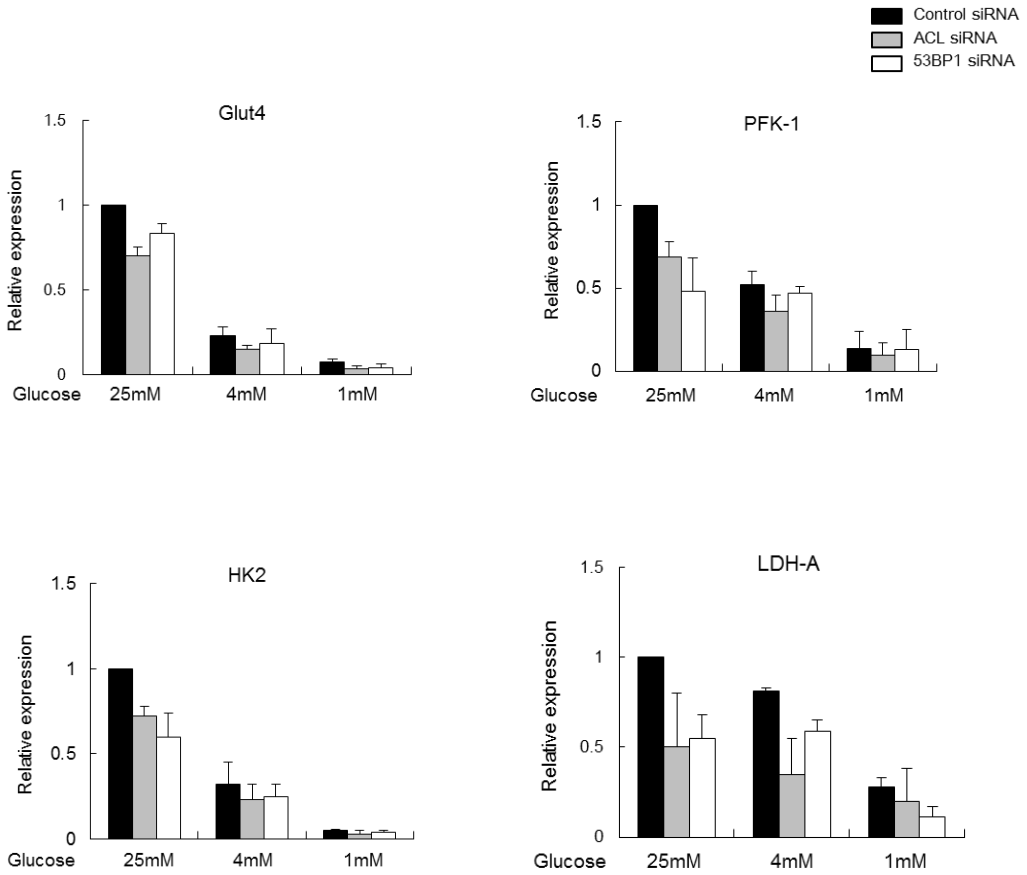


**Figure 10. Silencing of 53BP1 reduced histone acetylation in adipocytes**

3T3-L1 preadipocytes were transfected with control, 53BP1, and/or ACL siRNAs and 2 days later stimulated to differentiate into adipocytes. **(A)** Acid extracts from 3T3-L1 cells 4 days after induction of differentiation, analyzed by western blot. **(B)** Cells were fixed and Oil Red O lipid staining was performed 5 days after induction of differentiation. Similar results were obtained in each of 3 independent experiments. Western blot used total lysates. **(C)** Total lysates from 3T3-L1 cells 4 days after induction of differentiation, analyzed by western blot. **(D)** RNA was isolated 4 days after induction of differentiation. Gene expression was analyzed by Real-time PCR and normalized to GAPDH. **(E)** Acid extracts from 0 and 4 days after induction of differentiation in the presence of 1, 5, or 10mM sodium acetate were analyzed by western blot. **(F)** Oil Red O lipid staining was performed 5 days after induction of differentiation, with or without 1mM sodium acetate. **(G)** RNA was isolated 4 days after induction of differentiation in the presence or absence of 1mM acetate. **(H)** Western blots of cells differentiated 4 days in 1mM, 4mM or 25mM glucose. **(I)** Gene expression in cells 4 days after induction of differentiation in 1, 4, or 25mM glucose was as-

essed by realtime PCR and normalized to GAPDH.

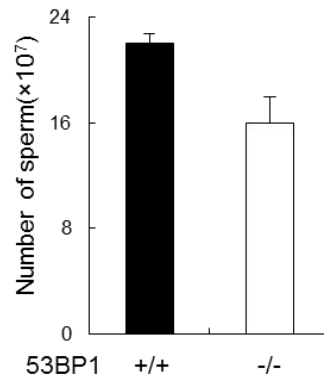
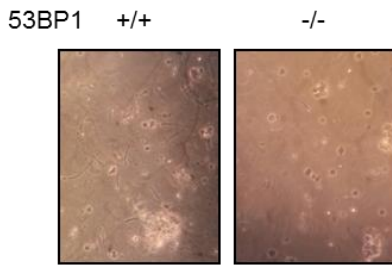
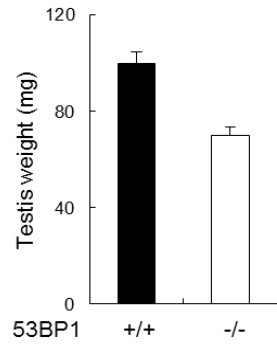
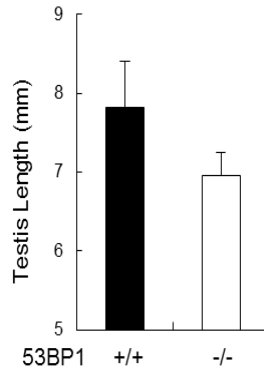
#### **iv. 53BP1 regulates histone acetylation during mouse spermatogenesis**

Mammalian spermatogenesis is a unique process with successive process with successive proliferation and differentiation, consisting of spermatogonial self-renewal, spermatocytic meiosis and spermiogenic chromatin remodeling [28], [29]. We choose spermatogenesis as a model system to investigate the level of histone acetylation.

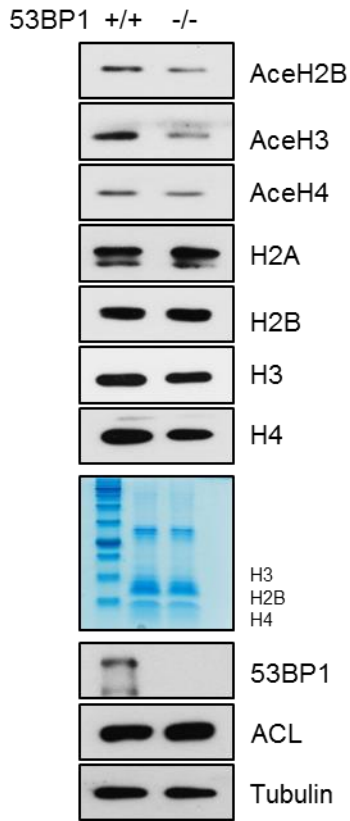
The data showed that length and weights of testes were lower in 53BP1 knockout-mice than those in control mice. Similarly, numbers of sperm were decrease in 53BP1 knockout-mice (Figure 11A). These data showed us 53BP1 may be necessary for development of testis. Global hyperacetylation of core histones, especially histone H4, is known to play an important role in the histone-to-protamine exchange during spermiogenesis [30]. To examine the effects of 53BP1 on histone acetylation, we lysate total protein from testes and used Histological examination of paraffin-embedded sections and immunohistochemistry to investigate the expression of histone H4 in control mice and 53BP1 knockout-mice. In the testes western bolt result, global histone acetylation H3, H4, H2B were decreased at 53BP1 knockout samples compared with that of control group (Figure

11B). Histological examination of the testes of 53BP1 knockout mice showed morphologically abnormal round spermatids characterized by detachment or sloughing into the lumen of the seminiferous tubules (Figure 11C). The result of immunohistochemistry of histone H4 acetylation that 53BP1 KO mice tests were mainly stained in spermatogonia. But WT mice testes were stained in spermatid, indicating that 53BP1 knockout mice were presented defect of spermatogenesis (Figure 11D). These data suggest that 53BP1 promotes spermatogenesis through histone acetylation.

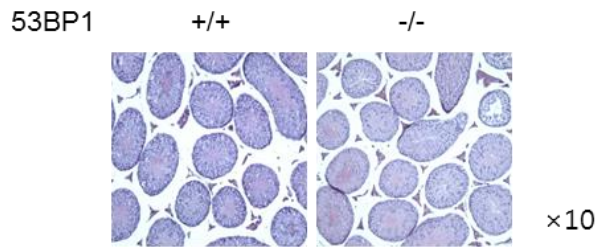
A



**B**



**C**



**D**

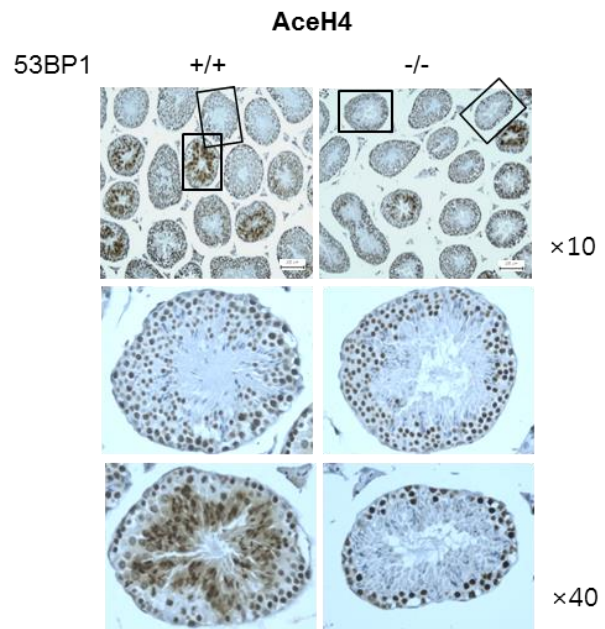


**Figure 11. Testicular development and spermatogenesis in 53BP1 knock out Mice**

(A) Analysis of overall size, weight, length of testes and the number of sperm from 10-week-old 53BP1 wild-type and knockout mice. (B) Total lysates from 10-weeks-old 53BP1 wild type and knockout mice analyzed by western blot. (C) Hematoxylin and eosin staining of 53BP1 wild-type mice and knockout testis. (D) Immunohistochemical detection of histone acetyl H4 with 53BP1 wild-type mice and knockout testis.

## 5. 53BP1 influences gene expression through histone acetylation

Histone modifications have been linked to a number of chromatin-dependent processes, including replication, DNA-repair, and transcription. Transcription proceeds in a series of steps, also referred to as initiation and thereafter elongating pol II, elongation, and finally termination [31], [32]. The first four steps take place at the promoter and are tightly regulated to achieve a precise control of gene expression. Acetylation of nucleosomal histones is a major determinant of chromatin structure and gene activity, with the degree of histone acetylation correlating with gene transcription. In this study, we showed that 53BP1 regulates histone acetylation. To explore 53BP1 function in gene expression through histone acetylation, we performed RNA-seq. experiments using 53BP1 WT and 53BP1 KO MEF cells.

To analyze differentially expressed genes (DEGs) that related to 53BP1, all sequenced genes were screened between 53BP1 WT and KO cells. Figure 12A showed different expression levels between 53BP1 WT and KO cells by expression fold-change (>2 fold) and student's t-test ( $P < 0.01$ ). A total of 2162 DEGs were identified in the transcriptomic comparison (Figure 12A), comprising

1587 upregulated and 575 downregulated DEGs. To determine the functions of DEG, we used the KEGG(Kyoto Encyclopedia of genes and enomes) enrichment analysis. The functional classification of DEGs was generalized as biological process, cellular process, and molecular function, and 2006 genes were annotated in several pathways (Figure 12B). We confirmed downregulated DEGs mRNA expression levels of the 53BP1 WT type and 53BP1 KO type cells use real-time PCR and selected genes all decreased in 53BP1 KO cell (Figure 12C). To further explore the gene expression by histone acetylation, we performed chromatin immunoprecipitation experiments revealed that acetylation of histone H3 at the target genes promoter was specifically reduced upon 53BP1 silencing, although, there have some genes like FANCD2, FANCI and EMEI did not decreased (Figure 12D). For recovery experiment, we transfected with siRNA control or 53BP1 to knockdown the gene, then transfected with HA vector or HA-53BP1 full length plasmid. The particular genes were recovered at 53BP1 full length plasmid transfected sample (Figure 12E).

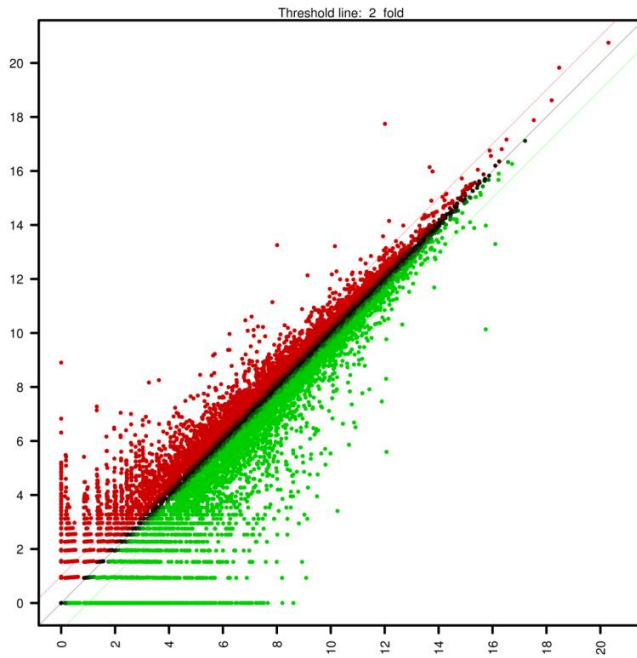
**Table 2. Deep Sequencing Data of 53BP1 Wild and Knockout Type Cells**

	TranscriptName	Gene_symbol	Gene Full Name	FPKM_PMEF-WT	FPKM_PMEF-KO
<b>Replication</b>	NM_008564	Mcm2	minichromosome maintenance deficient 2 mitotin (S. cerevisiae)	19.33	10.38
	NM_008563	Mcm3	minichromosome maintenance deficient 3 (S. cerevisiae)	18.43	10.59
	NM_008565	Mcm4	minichromosome maintenance deficient 4 homolog (S. cerevisiae)	19.01	11.32
	NM_001302540	Mcm5	DNA replication licensing factor MCM5	2.30	0.96
	NM_008567	Mcm6	minichromosome maintenance deficient 6 (MIS5 homolog, S. pombe) (S. cerevisiae)	28.04	13.44
	NM_008568	Mcm7	minichromosome maintenance deficient 7 (S. cerevisiae)	28.85	15.46
	NM_008892	Pola1	polymerase (DNA directed), alpha 1	3.70	1.66
	NM_008921	Prim1	DNA primase, p49 subunit	7.06	3.19
	NM_011132	Pole	polymerase (DNA directed), epsilon	3.40	1.66
	NM_011133	Pole2	polymerase (DNA directed), epsilon 2 (p59 subunit)	3.74	1.76
<b>Gene Regulation</b>	NM_001166537	Hnga1	high mobility group AT-hook 1	9.32	12.14
	NM_001164042	Smad5	SMAD family member 5	1.44	0.38
	NM_001110216	Cbx5	chromobox 5	2.01	0.79
	NM_001164080	Timeless	timeless circadian clock 1	0.67	0.57
	NM_001170967	Wdr33	WD repeat domain 33	0.01	0.00
<b>RNA Metabolism</b>	NM_001048267	Trnp1	transportin 1	2.40	0.80
	NM_001256117	Sun1	Sad1 and UNC84 domain containing 1	0.78	0.12
<b>FANCONI ANEMIA</b>	NM_001111078	Uhrf1	ubiquitin-like, containing PHD and RING finger domains, 1	7.49	5.55
	NM_053081	Fancg	Fanconi anemia, complementation group G	2.65	2.42
	NR_028297	Fance	Fanconi anemia, complementation group E	1.24	1.25
	NM_001033244	Fancd2	Fanconi anemia, complementation group D2	1.72	1.76

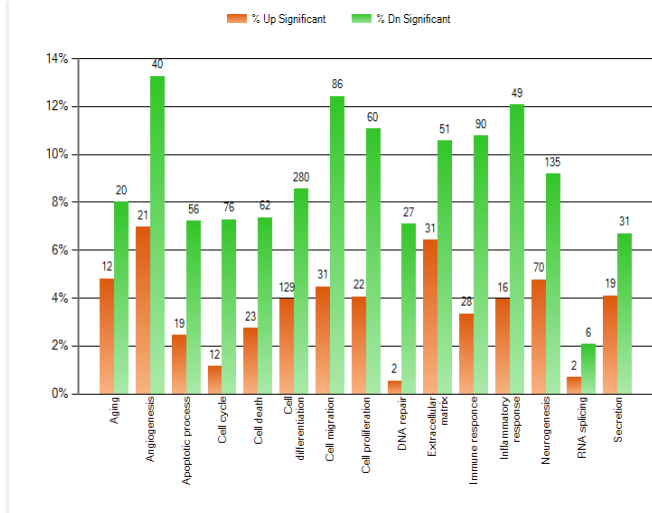
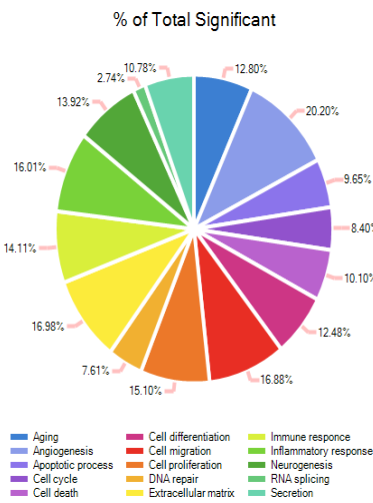
Table 2-1. Deep Sequencing Data of 53BP1 Wild and Knockout Type Cells

TranscriptName	GeneName	Gene Full Name	FPKM_PMEF-WT	FPKM_PMEF-KO
NM_001081324	Neto2	neuropilin (NRP) and tolloid (TLL)-like 2	3.33	1.55
NM_011172	Prodh	proline dehydrogenase	0.99	0.28
NM_177372	<b>Dna2</b>	DNA replication helicase 2 homolog (yeast)	2.68	0.86
NM_001167885	Suv420h1	suppressor of variegation 4-20 homolog 1 (Drosophila)	1.40	0.35
NM_016919	Col5a3	collagen, type V, alpha 3	38.23	7.47
NM_026056	Cap2	CAP, adenylate cyclase-associated protein, 2 (yeast)	7.48	3.44
NM_010097	Sparcl1	SPARC-like 1	0.59	0.24
NM_011495	<b>Plk4</b>	polo-like kinase 4 (Drosophila)	8.94	4.41
NM_144516	Zmynd11	zinc finger, MYND domain containing 11	7.49	3.26
NM_008813	Enpp1	ectonucleotide pyrophosphatase/phosphodiesterase 1	9.41	4.32
NM_001025613	Otud7b	OTU domain containing 7B	2.02	0.67
NM_001081323	Mphosph9	M-phase phosphoprotein 9	0.23	0.10
NM_011477	Sprr2k	small proline-rich protein 2K	26.68	3.33
NM_001142732	Tlll3	tubulin tyrosine ligase-like family, member 3	0.94	0.42
NM_009704	Areg	amphiregulin	1.29	0.16
NM_001109973	Mdfl	MyoD family inhibitor	0.49	0.21
NM_001081176	Poir3g	polymerase (RNA) III (DNA directed) polypeptide G	3.88	1.87
NM_134129	Psap	PRP19/PSO4 pre-mRNA processing factor 19 homolog (S. cerevisiae)	19.90	12.85
NM_001290445	Gpr154	G-protein coupled receptor 64 isoform 5 precursor	0.93	0.53
NM_001085472	Acin1	apoptotic chromatin condensation inducer 1	13.62	9.04
NM_138671	Nadk	NAD kinase	1.56	4.03
NM_001111078	Uhrf1	ubiquitin-like, containing PHD and RING finger domains, 1	3.81	8.38
NM_008960	Pten	phosphatase and tensin homolog	13.50	21.69

A

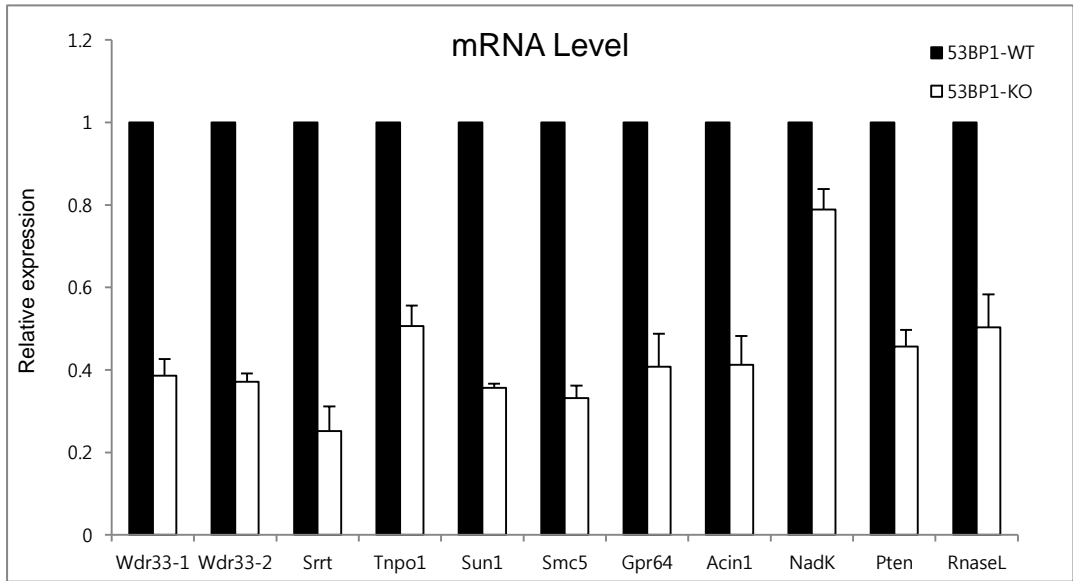


B

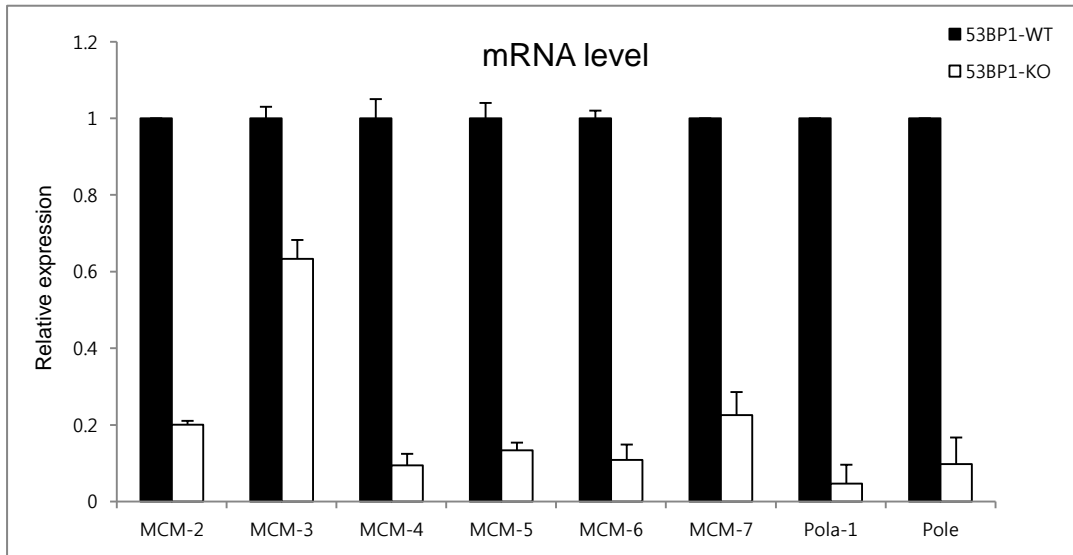


C

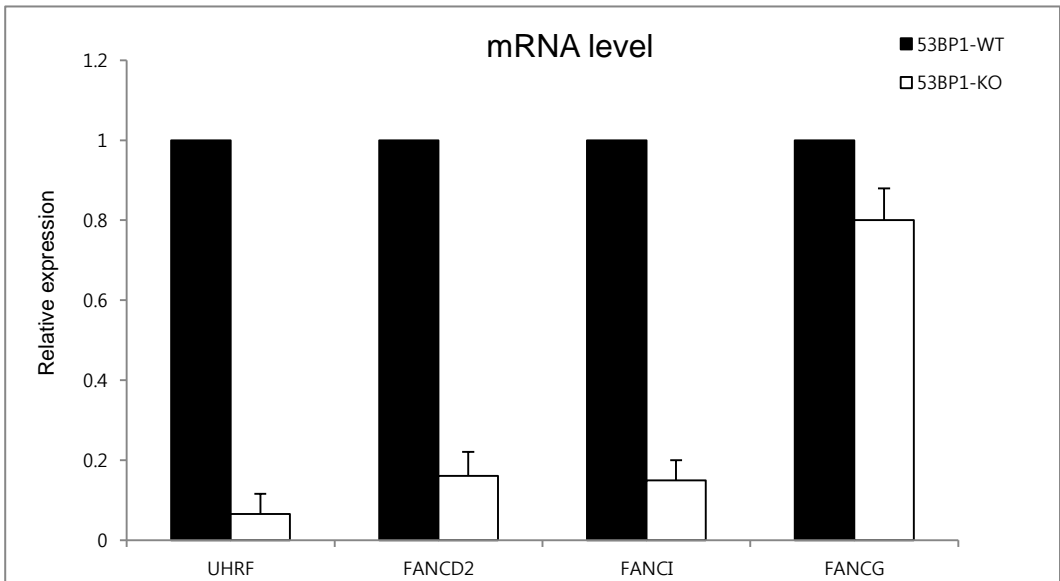
a



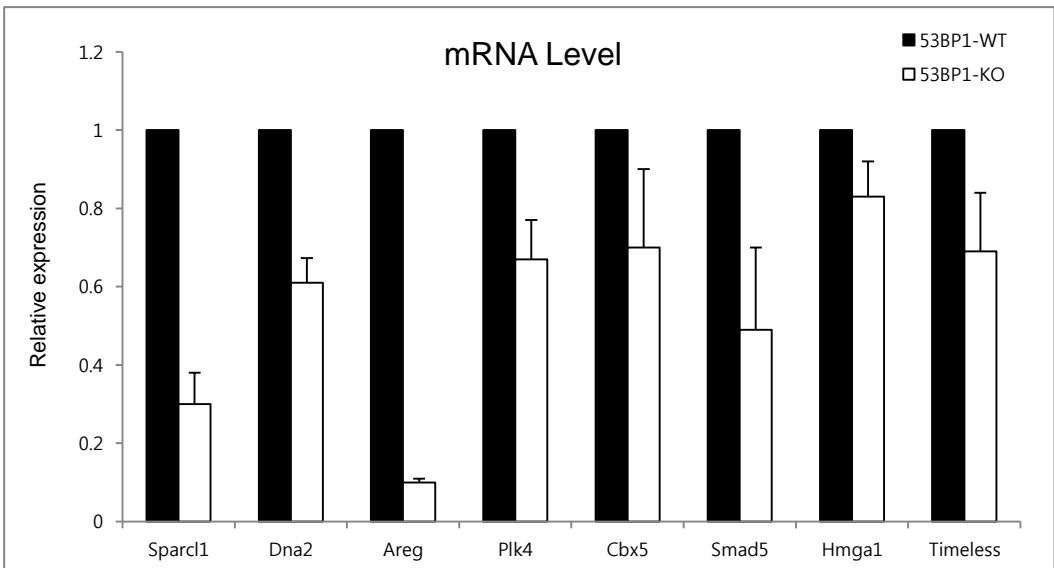
b



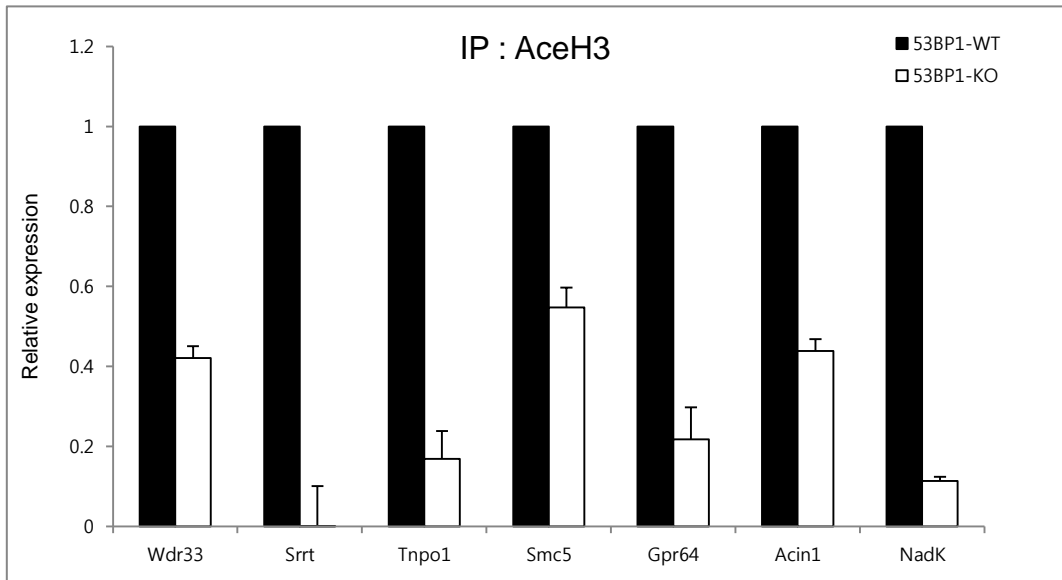
c



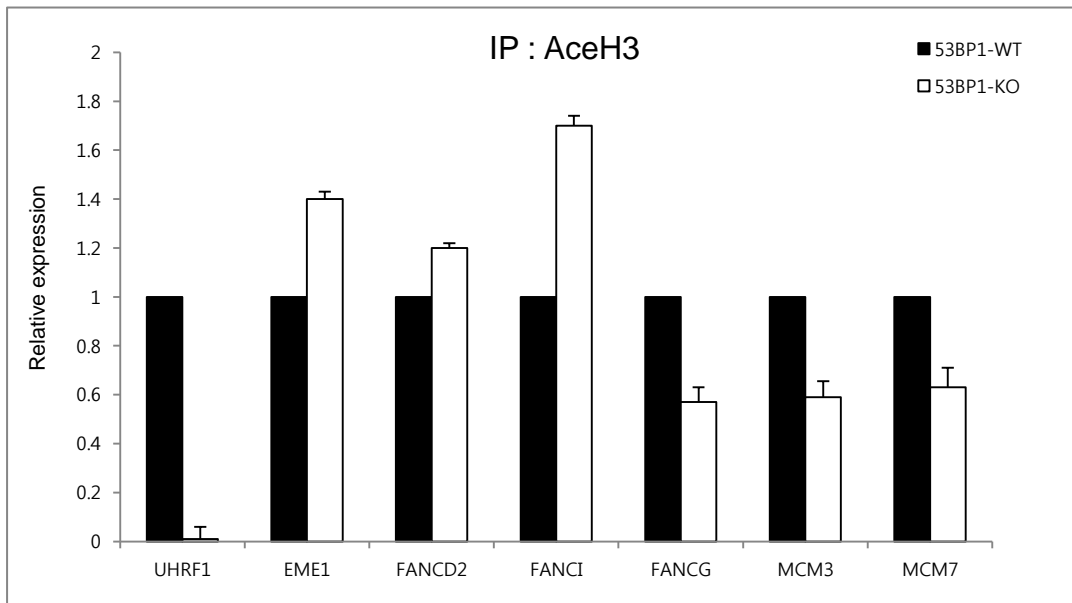
d



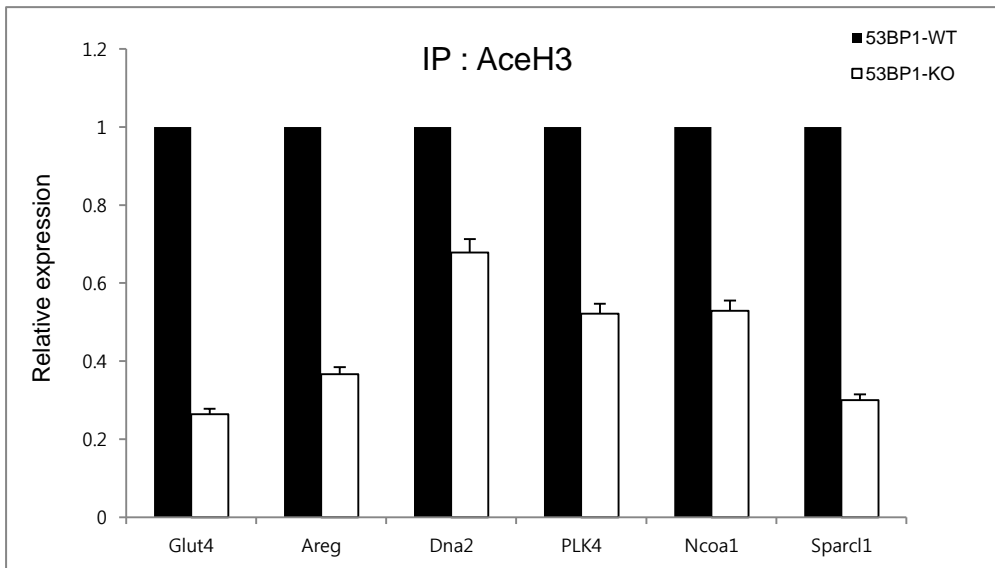
**D**  
**a**



**b**

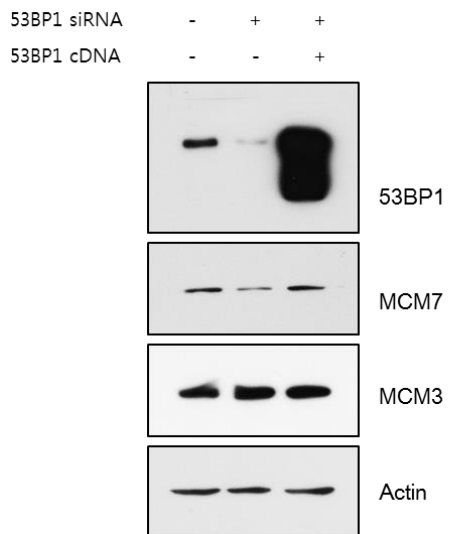


**c**



**C**

**a**



**b**

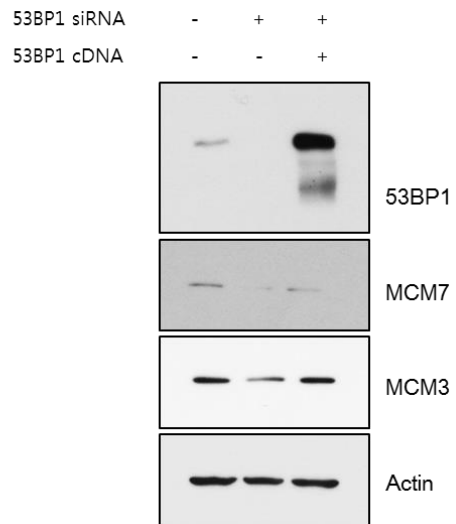


**Figure 12. 53BP1 influence gene expression through control histone acetylation**

(A) mRNA level confirm used primary MEF cell with or without 53BP1. Gene expression was analyzed by quantitative RT-PCR. (B) Chromatin immunoprecipitation was performed using antibody to histone Acetyl-H3. Immunoprecipitated target genes promoter sequence was analyzed by quantitative PCR. (C) Recovery experiment, used HEK 293T cell (a) and HELA cell (b).

**Table 3. Oligonucleotide Primer of the mRNA Real-time PCR**

Gene_symbol	TranscriptName	Primer sequene
Mcm2	NM_008564	F-GGAGCTCGATGTCTACGAGG
		R-ATCTTCCTCGCTGCTGTCAT
Mcm3	NM_008563	F-TGAGCAAGACTGTGGACCTG
		R-AATCGTCAGTCTTTGGGGTG
Mcm4	NM_008565	F-CTTTTTGCCACAATGACCT
		R-TTCACGTTGCTCACTCTTGG
Mcm5	NM_001302540	F-ACTGGATCGAGGTGGAGATG
		R-AGGGATCTTCACCAGGTGTG
Mcm6	NM_008567	F-TCACCCTGAGCTTGTGAGTG
		R-TGTTGGCACACACTGGATTT
Mcm7	NM_008568	F-CACTTGTGATCAGTGTGGGG
		R-CCCACAGGAAGTTGGTCACT
Pola1	NM_008892	F-ACCCTTTTTTCAGTGCACACC
		R-TTACCCCTAGCTCCTGCTCA
Prim1	NM_008921	F-GAATATGCCTTAGTCGGCCA
		R-GAGTTGGCCACTTTCCTCAG
Pole	NM_011132	F-GTACCAGACATTGAGGGCGT
		R-GTAGCTGAACTGGGCCAGAG
Pole2	NM_011133	F-GCTGAAAGCATCACACAGGA
		R-ACTGCTGCTAGGAAAACGGA

**Table 3-1. Oligonucleotide primer of the mRNA Real-time PCR**

Gene_symbol	TranscriptName	Primer sequene
Hmga1	NM_001166537	F-GAAAGAGCCCAGTGAAGTGC
		R-CTCCTCAGTGGCTATGGAGC
Smad5	NM_001164042	F-AGTCAACCATGGATTTCGAGG
		R-ACGTCCTGTCCGGTGGTACTC
Cbx5	NM_001110216	F-GAAGCTGACCTGGTTCTTGC
		R-GTGATGAGCGCAGTGGTTTA
Timeless	NM_001164080	F-CTGAGGCACGAGGATGAGAC
		R-AATGGTGCCGTACACTGGAG
Wdr33-1	NM_001170967	F-TTACAGTACACCAACCCGCA
		R-CTGACCAGAAAAGGGCTGAG
Wdr33-2	NM_001170967	F-AGTGGGGAGTTCACCTTGTG
		R-CGTTGTTTCATGTTGGATTGC
Tnpo1	NM_001048267	F-GTTCGGCAGAGTTCTTTTGC
		R-TTGCTGTGTTCTCCAACAGC
Uhrf1	NM_001111078	F-AGCTCCAGTGCCGTTAAGAC
		R-CGTTTCCTGGGGTAGTCCAC
Fancg	NM_053081	F-TACCTCGTCTCTGCTTCCCA
		R-TCACAGTCGGAGCCTTGTTTC
Fanci	NR_028297	F-CAAGAGCCGCTGGATCATCT
		R-TCCCATGATGAGACACGCAC

**Table 3-2. Oligonucleotide primer of the mRNA Real-time PCR**

Gene_symbol	TranscriptName	Primer sequene
Fancd2	NM_001033244	F-CAAAAGATGCCAGTCGAGCG
		R-GTTGTCTTGCCACGCAAAGT
EME1	NM_177752	F-GTCTAGCACGGGACTCATGG
		R-TCTTGAAGGGTGCTTCAGCC
Sun1	NM_001256117	F-CATGAAGTGCGTCTCTCCAA
		R-CCTGCTTTCAGCTTGGTTTC
Dna2	NM_177372	F-TTCGCAGATAGGCAACTGTG
		R-CTGGTGAGTCTTCCGGTTGT
Col5a3	NM_016919	F-GGTCCTCTCCTTCCATCCTC
		R-ATGCCTCTCGCACTGACTTT
Sparcl1	NM_010097	F-CCACATACAGAGCAGCAGGA
		R-TGGCTGGGGATGAAGTAGTC
Plk4	NM_011495	F-AAACCAAAAAGGCTGTGGTG
		R-GGAGGTCTGTCAGCAAGAGG
Areg	NM_009704	F-CATTATGCAGCTGCTTTGGA
		R-GCCGGATATTTGTGGTTCAT
Gpr64	NM_001290445	F-CTGTGGTTGTGTCCATCGTC
		R-CACCACATTGCTGTTGATCC
Acin1	NM_001085472	F-GCAGACCAAGTCAGCAATGA
		R-CCCCCTCTGTGTCACTGTTT

**Table 3-3. Oligonucleotide primer of the mRNA Real-time PCR**

Gene_symbol	TranscriptName	Primer sequene
Nadk	NM_138671	F-CTGGCTGACCTAGCCTTGAC
		R-CTGACCCCCTCAGAATTTCA
Pten	NM_008960	F-CCTGCAGAAAGACTTGAAGGTG
		R-TGCAGTTAAATTTGGCGGTGTC
Glut4	NM_009204	F-CTGTCGCTGGTTTCTCCAAC
		R-GCATCCGCAACATACTGGAA
Pfk-1	NM_001163488	F-TCTCTAAGGGTGGGTTGCAC
		R-CCATCATGTACGACCAGCAC
Hk2	NM_013820	F-CTGTCTACAAGAAACATCCCCA
		R-CACCGCCGTCACCATAGC
LDH-A	NM_010699	F-AGACAAACTCAAGGGCGAGA
		R-GCGGTGATAATGACCAGCTT
ap2	NM_011547	F-TCACCTGGAAGACAGCTCCT
		R-AATCCCCATTTACGCTGATG
Cebp	NM_001287738	F-AGGTGCTGGAGTTGACCAGT
		R-CAGCCTAGAGATCCAGCGAC
PPAR-r	NM_011144	F-GGTGAAACTCTGGGAGATTC
		R-CAACCATTGGGTCAGCTCTT
Srrt	NM_001109909	F-AACTGAGTCCCGGTGTGAAC
		R-CGCACTCACTTCCTCAATCA

**Table 4. Promoter primer of the Chip assay**

Gene_symbol	TranscriptName	Primer sequene
Mcm3	NM_008563	F-GGTTTTGAGCGTCCTCTCTG
		R-CGGAAGTTTATGGTGGAGGA
Mcm7	NM_008568	F-GCGACACAGACTGATCTGGA
		R-GTGTTTCTTAAAGCGCCAGC
Uhrf1	NM_001111078	F-GCTAAAGTTCGCGGGAAACG
		R-TGCGATTGGCCTAGATGACC
Fancg	NM_053081	F-TCTTTTCTTGGGCGTTCTCCA
		R-TTAGAACCAACGGCAGTCCA
Fanci	NM_145946	F-TCAGACCTCCTAGCTGCCTT
		R-CGACAGTACGGGAAAGGAGG
Fancd2	NM_001033244	F-ACAGTCGTATGCACAGGCAA
		R-ACCTGTAGGTGGAGCAGTGA
EME1	NM_177752	F-GCTCAGTGGGTAAGAGCACC
		R-GAAGAGGGCGTCGGATCTTG
Hmga1	NM_001166537	F-ATGCAAGGTCTTTGGGATTG
		R-TTAGCGGCTTGGTCTGTTCT
Smad5	NM_001164042	F-GTTGCTCAGACTGGACGTGA
		R-TCCTGATGATGACAGGTGGA
Cbx5	NM_001110216	F-AGTCAGGTGCATTGTAGGGG
		R-CACCTTTCATCCCAGCACTT

**Table 4-1. Promoter primer of the Chip assay**

Gene_symbol	TranscriptName	Primer sequene
Timeless	NM_001164080	F-TGTGGCCCAGGCCTTAATTC
		R-ATCTGCTAGCCCCAGGAAA
Wdr33	NM_001170967	F-AGCTTGATCTCCAGCCTTCA
		R-TGCAAATTGGGTTCTCTCC
Tnp01	NM_001048267	F-GTTTCGCAGGGGTTTTGATA
		R-AGTCACGGACAGTGAAACCC
Srrt	NM_001109909	F-ACCCTCTCCCGTCATTCTT
		R-GACCACAAAGAGGGTTGGAA
Dna2	NM_177372	F-CCTTGTTTTGATGGCTTGGT
		R-GCCAGCCTTGGTCTACAGAG
Col5a3	NM_016919	F-GGTCCTCTCCTTCCATCCTC
		R-ATGCCTCTCGCACTGACTTT
Sparcl1	NM_010097	F-TTCCCTAGTATGGTCGTGGG
		R-GGGAGATGGTTCCTGTGTGT
Plk4	NM_011495	F-ATGGACTGACTCAACCCCAG
		R-CGTTGTGCCATTTTCCTTTT
Areg	NM_009704	F-CACGCCCAGCTAAAACCTTA
		R-TAGCCCGAAGACTTTGAGGA
Gpr64	NM_001290445	F-TTAGTACCAGCCCTTGGTCG
		R-CTGCCAGGTAATGTCAGGGT

**Table 4-2. Promoter primer of the Chip assay**

Gene_symbol	TranscriptName	Primer sequene
Acin1	NM_001085472	F-GCTACATGGCTTCCATGGTT
		R-CTTCCAAGGGGAAAAGGAAG
Nadk	NM_138671	F-CAGACCCCAGTGCATAACCT
		R-CACCCCTCACTGGTGTCTTCT
Pten	NM_008960	F-GGAGAGTTGCTCTCTCCCCT
		R-GAAGACGGATAATCCTCGCA
Glut4	NM_009204	F-CCTGACATTTGGCGGAGCTAA
		R-TATGTGTGTATGCCCCGAAG
Smc5	NM_145498	F-AGTTCATTTGAGCACCAGGG
		R-CTCAGAGGTGCGATGTGTGT
Ncoa1	NM_010881	F-GATCAAGGCTCAAGGAGCTG
		R-AGAAAGATCATCTGCCCCCT

## **6. Novel function of 53BP1 by histone acetylation mediated gene expression decrease**

In the figure 11, through comparison and confirm of results across RNA sequencing technology, we found that 53BP1 is correlate with lots of gene expression. Furthermore, chromatin immunoprecipitation experiments revealed that acetylation of histone H3 at the target genes promoter was specifically reduced upon 53BP1 silencing. We selected Dna2, Plk4, MCM3 and MCM7 for further examination.

### **i. Downregulation of Dna2 in 53BP1-deficient cells**

Dna2 is an evolutionarily conserved helicase/nuclease enzyme, hDna2 localizes to the mitochondria and participates in mtDNA replication and repair [33], [34]. We speculated that 53BP1 through regulate Dna2 gene expression would abrogate mtDNA repair. To assess mtDNA repair, DNA from cells expressing a control RNAi hairpin or cells expressing a hairpin targeting h53BP1 was isolated following H<sub>2</sub>O<sub>2</sub> treatment. Lesions in mtDNA were assessed by PCR amplification of an 8.9-kb fragment of mtDNA and normalized to mtDNA copy number by using a shorter mtDNA PCR

product (221 bp). Analysis of mtDNA 0, 1, 4, and 8 h after H<sub>2</sub>O<sub>2</sub> treatment revealed that 53BP1 depletion resulted in a significant reduction in the repair of oxidative lesions within the mtDNA (Figure 13A). These results suggest a potential role for 53BP1 in mtDNA repair and replication via upregulation of Dna2 expression.

## ii. Decrease of plk4 in 53BP1-deficient cells

Plk4, Polo-like kinase family member, has been established as a conserved key regulator of centriole formation. Loss of Plk4 prevents centriole formation and its overexpression leads to de novo formation of centrioles in both unfertilized *Drosophila* eggs as well as in *Xenopus*-activated oocytes and extracts [35], [36]. Centrosome abnormalities are more severe in high-grade and recurrent tumors and in cell lines that show aggressive malignant phenotypes [37]. In mitosis, supernumerary centrosomes can lead to an increase in spindle poles, and multipolar spindles are found in many cancer cell types [38]. Here, to test whether the silencing of 53BP1 was the cause of the change in spindle-associated dynein. We used immortal 53BP1 WT or KO MEF cell and demonstrated that in 53BP1 knockout cell line, multipolar spindle was increased (Figure 13B). Thus, we demonstrated

that 53BP1 regulates centriole duplication and may represent a new mitosis regulator.

### **iii. Reduction of MCM3 and MCM7 in 53BP1-knockdown cells**

Minichromosome maintenance (MCM) proteins 2–7 are important in DNA replication licensing [39]. Functional roles beyond licensing are speculated. FANCD2 is a general effector of ATR signaling that targets stalled replication forks and associates with MCM2–MCM7 hexamers upon DNA replication stress [40]. Recently studies showed Dna2-dependent processing of reversed forks—leading to ssDNA stretches on the regressed arms—which appear to promote efficient fork restart [41]. Our RNA sequencing screening data showed silencing of 53BP1, replication associate genes: Dna2, MCM3 and MCM7 expression decreased. So, To begin elucidating the role of 53BP1 during replication stress, we monitored replication perturbation by genome-wide single-molecule DNA fiber replication assays. We measured whether 53BP1 through regulate Dna2 expression to process stalled replication intermediates by monitoring the integrity of the newly synthesized DNA after HU treatment. To this purpose, We first pulsed U2OS cells with IdU for 60 min, and then varied the exposure time to HU from 6 h. The mean length of the IdU tracts progressively during HU

treatment is 18.2  $\mu\text{m}$  (8 h) However, shRNA-mediated 53BP1 depletion largely prevented IdU tract shortening, confirming that 53BP1 is responsible for the observed nascent strand degradation (Figure 13C-a). Next, we tested the stability of nascent DNA in U2OS cell deprived of nucleotides for a long period of time. HDFs were pulse labeled with CldU for 2 hr in the presence of HU and maintained in HU-containing medium for 16 hr before DNA fiber preparation. The mean length of CldU tracks in 53BP1-depleted cells was now shorter than CldU tracks from cells treated with the control siRNAs. Suggesting that CldU tracts were trimmed in 53BP1-depleted cells during the 16 hr incubation period in HU (Figure 13C-b). we therefore conclude that 53BP1 is required for the maintenance of replication fork stability after HU.

**A**

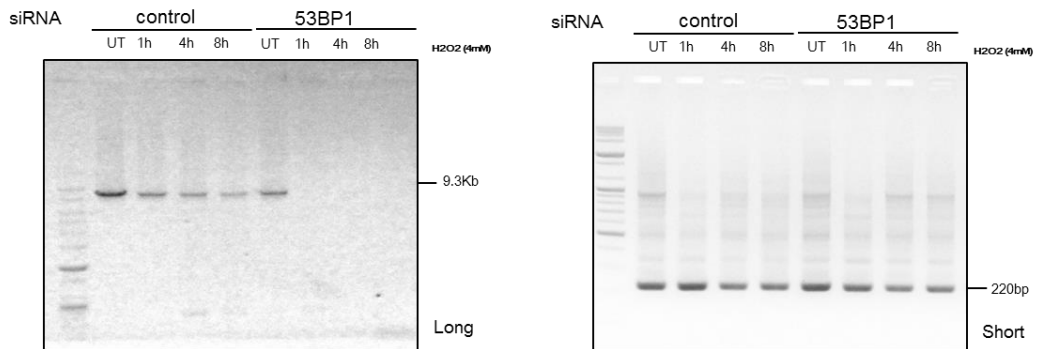
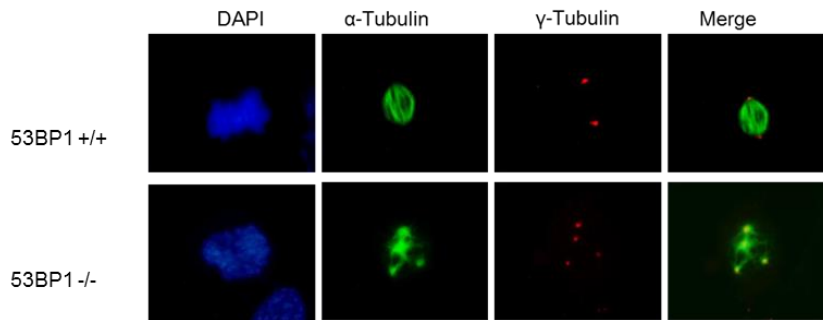


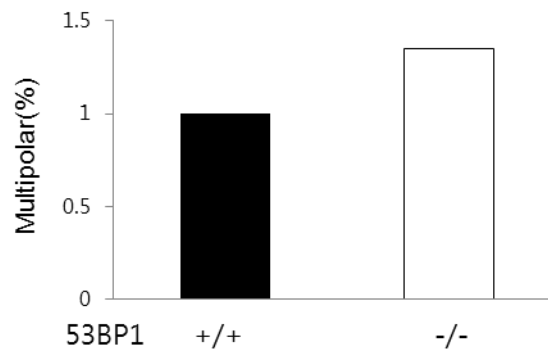
### Figure 13. Preparatory experiments of 53BP1 new functions

(A) RT-PCR of DNA extracted from U2OS cells expressing siCTL and si53BP1. Cells were treated with 2mM H<sub>2</sub>O<sub>2</sub> and allowed to recover for 0, 1, 4, or 8h. (B) The staining used immortal MEF cell with or without 53BP1, the percentage of multipolar form are indicated. (C) a. Representative DNA fiber image (top), Representative IdU tract length distributions during different exposure time to HU (out of 3 repeats; n>300tracts scored for each dataset).b. cell were synchronized by serum starvation for 24hr, released in presence of serum, and labeled in S phase for 20min with IdU and then for 2hr with CIIdU in the presence of 5mM HU. And washed and maintained in HU-containing medium for 16hr. CIIdU tracks measured in  $\mu$  m.

**B**



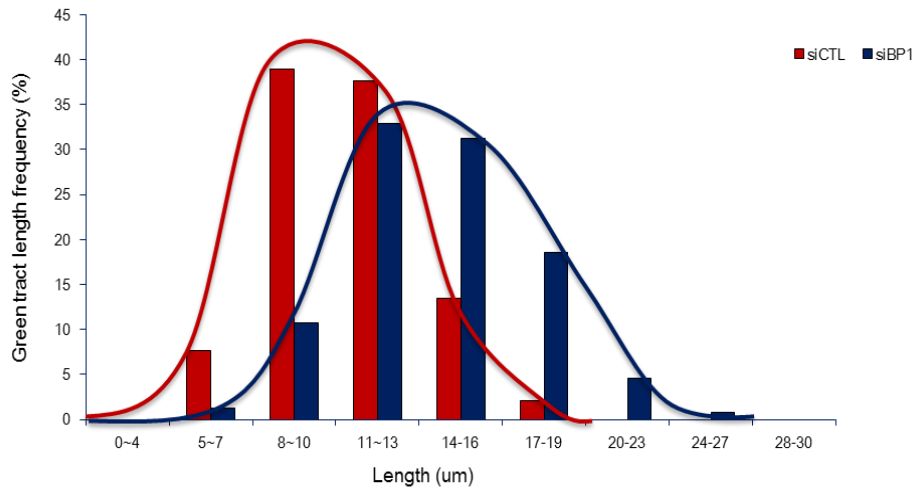
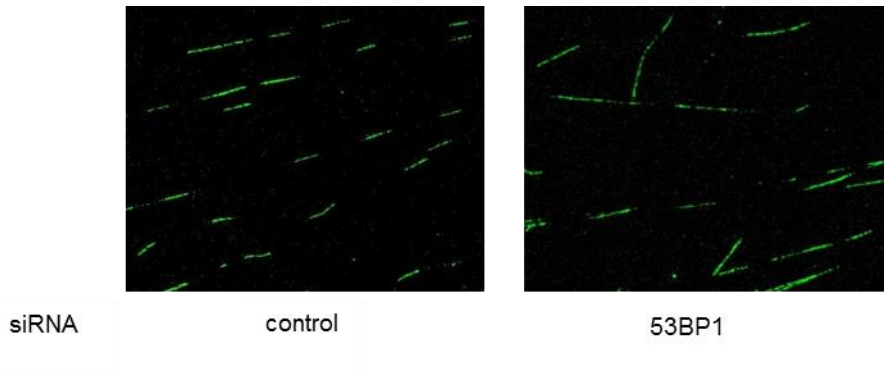
Cell type	Total cell	Normal	Multipolar
53BP1+/+	50	40	10
53BP1-/-	37	27	10



**Immortal MEF cell**

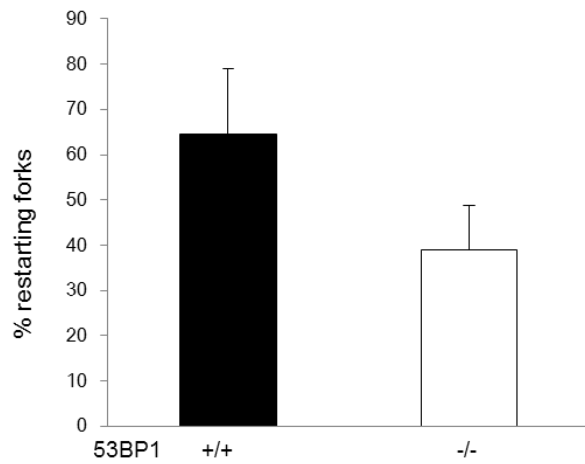
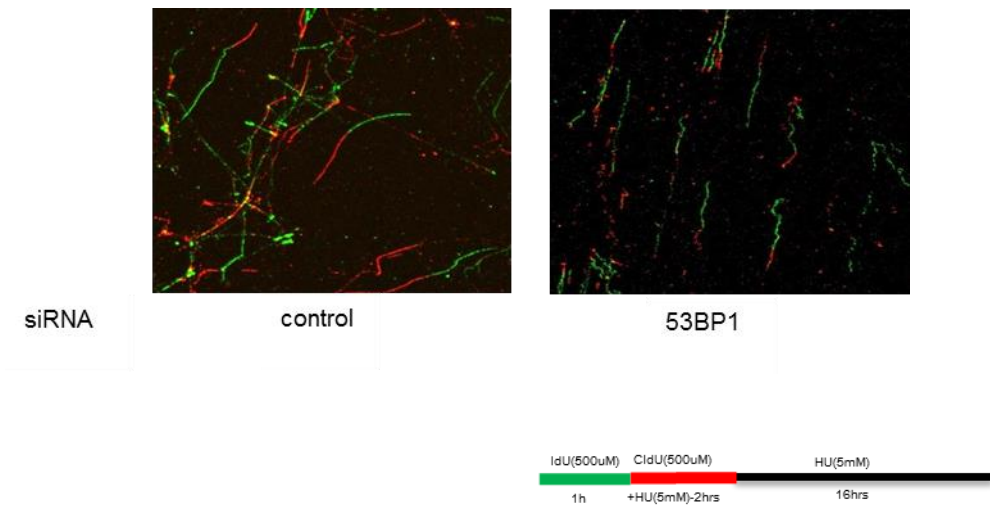
**c**

C  
a



HeLa cell

b



HeLa cell

## DISSCUSSION

The findings of this study demonstrate that 53BP1 regulates ACL activity, lipid synthesis, histone acetylation through interaction with ACL.

### 1. 53BP1 regulates ACL activity by interacting with ACL

Protein-protein interactions play crucial roles in the execution of various biological functions [42].

We previously developed the unknown 53BP1 interacting protein used yeast two-hybrid screening for human. Metabolism enzyme ACL was found interacting strongly at N-terminal (a.a 1-699) of 53BP1. Then we confirmed 53BP1 interaction with ACL both in vivo and in vitro.

We confirmed that 53BP1 interacts with ACL in vivo, using endogenous and exogenous co-Immunoprecipitation. We also showed that ACL specific interacts with 53BP1 N-Terminal but not C-Terminal. Through GST full down assay, We confirmed that ACL directly interacts with 53BP1 N-terminal fragment. To identify binding domain between 53BP1 and ACL, we used eight 53BP1 fragment, and found that binding site of ACL is region 53BP1 N-terminal (a.a 1-100) and (a.a 301-

699). To determine whether 53BP1 affects the activity of ACL, we performed ACL activity assay.

found that 53BP1 upregulated ACL enzymatic activity, in particular in the N-terminal domain.

ACL activity is the most important point of this report, so In the future, more work is need both to

understand the mechanisms of how 53BP1 regulates ACL activity through binding with it. And we

conjecture two ways to influence ACL activity. One is through binding domain: ACL protein con-

tains five functional domains, named from N-terminus domains 3, 4, 5, 1 and 2. Domain 1 binds

CoA and domain 2 contains a phosphorylation site His765, regulating enzyme activity [43]. And

another way is through acetylation of ACL. Recently, report showed that ACL is acetylated at ly-

sine residues 540, 546, and 554 (3K). And these acetylation sites stabilize ACL activity [44]. In

case, 53BP1 binding with regulating ACL enzyme activity domain or through binding with 53BP1,

3K acetylation of ACL is increased, these effects should be an important point of 53BP1 regulates

ACL activity mechanism.

## 2. Deletion of 53BP1 leads to decreased histone acetylation

Histone acetylation can be divided into two groups, ACL dependent (acetyl-CoA/HAT) and ACL independent (HDCA inhibition) [45]. We have demonstrated that 53BP1 plays a critical role in determining the ACL dependent histone acetylation in multiple mammalian cell types and various cell conditions. First, in maintenance of histone acetylation, after knockout or knockdown 53BP1, decreased the amount of histone acetylation for all core histone assessed, and this decrease can be recovered after overexpression with 53BP1 plasmid. In conventional reports, serum induced changes in histone acetylation were dependent on glucose and failed to occur in absence of ACL. So we used 53BP1 knockout cell to confirm if correspond with ACL. The data showed silencing of 53BP1 inhibits histone acetylation after serum stimulation and glucose induction. Then we also observed histone acetylation during differentiation of murine 3T3-L1 preadipocytes into adipocytes in 53BP1 deficient cells. Histone acetylation was regulated during differentiation by 53BP1, and glucose-dependent regulation of histone acetylation was dependent on 53BP1. Similarly, the expression of carbohydrate metabolism genes in an 53BP1-dependent manner also. These patterns

agreement with ACL. So we convinced through regulate ACL activity, 53BP1 plays important roles on ACL dependent histone acetylation. Last, we used mouse model, and through testicular development and spermatogenesis assay confirmed 53BP1 regulates histone acetylation certainly.

In the Figure 8 data showed that in 53BP1 silencing cell not only global histone acetylation was decreased, to specific histone acetylation also had impact. Acetylation of histone located at DSB repair sites by histone acetyltransferases (HATs) is a critical chromatin modification required for DSB repair. In particular, the N-terminal lysine residues of histones H3 and H4 are acetylated during DSBs [46], [47]. Recently, much reports showed that DSB-induced acetylation of lysine 5, 8,12 and 16 within histone H4 and DNA damage-induced acetylation of N-terminal lysines 9,14,18,23 and 56 with histone H3 in mammalian cells were observed [48]. 53BP1 as a mediator/adaptor of the DNA-damage response, and is recruited to nuclear structures termed foci following genotoxic insult [49]. In the future, that should be interesting to consider that how can 53BP1 the relative roles of specific histone acetylation after DNA damage. And the influence of these residues must be also addressed, as well as the functional relationship between 53BP1 and other DDR components.

### 3. 53BP1 regulates gene expression through control of histone acetylation

Gene expression is in part regulated by differential acetylation of nucleosomal histones resulting in either transcriptional activation (hyperacetylation) or repression (hypoacetylation) [50], [51]. In this study, we showed 53BP1 can influence histone acetylation. To research the differential gene expression by 53BP1, RNA-Seq was performed. We confirmed RNA-Seq data with mRNA realtime PCR, and to identify whether the expression level changes in 53BP1 knockout cell associated with histone acetylation, chromatin immunoprecipitation experiment was proceed, the results revealed that acetylation of histone H3 at the various target genes promoter were specifically reduced upon 53BP1 silencing. The target genes include RNA metabolism relevant genes: Wdr33, Srrt and Tnp1; DNA repair, cancer, cell death and ROS regulation relevant genes: Smc5, Gpr64, Acin1 and Nadk; mtDNA replication and repair relevant gene Dna2, centriole biogenesis relevant gene Plk4 and DNA replication relevant genes MCM3, MCM7 and Dna2 and We selected Dna2, MCM3, MCM7 and Plk4, for further examination.

MCM proteins were first identified in the yeast *Saccharomyces cerevisiae* as mutants defective

in the maintenance of minichromosomes, suggesting a role in DNA replication. Six of them (MCM2–7) are related to each other and interact to form a stable heterohexamer in solution and form a family of DNA helicases implicated at the initiation step of DNA synthesis [52], [53], [54].

DNA2 is a highly conserved nuclease/helicase initially identified in *Saccharomyces cerevisiae* screening for mutants deficient in DNA replication [56], [57]. And human DNA2 seems to play a partially redundant role with human exonuclease I (EXO1) in replication-coupled repair [58], whereas a recent study in *S. pombe* suggested that the nuclease activity of Dna2 is required to prevent stalled forks from reversing upon HU treatment [59]. Additionally, the mitochondrial localization of hDna2 suggests a role for hDNA2 in mitochondrial DNA replication and repair. As well, hDna2 may provide helicase activity to unwind the DNA duplex during mtDNA replication.

We speculated that 53BP1 through regulate Dna2 gene expression would abrogate mtDNA repair and DNA fiber analysis suggests that 53BP1 degrades stalled replication intermediates beyond the maximum length of the reversed arms measured. And the mean length of CldU tracks in 53BP1-depleted cells was now shorter than CldU tracks from cells treated with the control siRNA, sug-

gesting that CldU tracts were trimmed in 53BP1-depleted cells during the 16 hr incubation period in HU. These results were coincide with silencing Dna2 and Fancd2.

Plk4 activity is essential for duplication of the centrosome, the cells major microtubule organizing center[60], its overexpression resulted in centriole amplification; conversely, RNA interference (RNAi) of the Plk4 gene caused the sequential reduction of centriole number [61],[62]. Our result revealed that acetylation of histone H3 at the Plk4 gene promoter was specifically reduced upon 53BP1 silencing. So we used immortal MEF cell with or without 53BP1, demonstrated that in 53BP1 knockout cell line, multipolar spindle was increased. This result coincide with recently study [63].

The previous studies revealed that 53BP1 is not only a critical regulator of mammalian DSB repairs but also it has emerged as potent antagonist of BRCA1 protein [64]. Recently, regulatory role of 53BP1 in mitosis was reported [18]. In this study we concluded, 53BP1 is a novel interacting partner of enzyme ACL and functionally involved in regulate enzyme activity influence on ACL-dependent histone acetylation and affect glucose-dependent lipogenesis. New functions of 53BP1

were identified. Moreover, through effect gene expression, 53BP1 was proved association with

mtDNA and nDNA replication, in the future we will research this area of 53BP1 concretely.

## REFERENCES

1. Xu, J.S., et al., Hepatic Carboxylesterase 1 Is Induced by Glucose and Regulates Postprandial Glucose Levels. *Plos One*, 2014. **9**(10).
2. Rodgers, J.T. and P. Puigserver, Fasting-dependent glucose and lipid metabolic response through hepatic sirtuin 1. *Proceedings of the National Academy of Sciences of the United States of America*, 2007. **104**(31): p. 12861-12866.
3. Hatzivassiliou, G., et al., ATP citrate lyase inhibition can suppress tumor cell growth. *Cancer Cell*, 2005. **8**(4): p. 311-21.
4. Wellen, K.E., et al., ATP-citrate lyase links cellular metabolism to histone acetylation. *Science*, 2009. **324**(5930): p. 1076-80.
5. Rathmell, J.C. and C.B. Newgard, Biochemistry. A glucose-to-gene link. *Science*, 2009. **324**(5930): p. 1021-2.
6. Toto, P.C., P.L. Puri, and S. Albini, SWI/SNF-directed stem cell lineage specification: dynamic composition regulates specific stages of skeletal myogenesis. *Cell Mol Life Sci*, 2016. **73**(20): p. 3887-96.
7. Kornberg, R.D., Chromatin structure: a repeating unit of histones and DNA. *Science*, 1974. **184**(4139): p. 868-71.

8. Biterge, B., A Mini Review on Post-Translational Histone Modification. *MOJ. Cell Sci. Rep.*, 2016. **3**(1).
9. Bannister, A.J. and T. Kouzarides, Regulation of chromatin by histone modifications. *Cell Research*, 2011. **21**(3): p. 381-395.
10. Allfrey, V.G., R. Faulkner, and A.E. Mirsky, Acetylation and Methylation of Histones and Their Possible Role in the Regulation of Rna Synthesis. *Proc Natl Acad Sci U S A*, 1964. **51**: p. 786-94.
11. Kleff, S., et al., Identification of a gene encoding a yeast histone H4 acetyltransferase. *J Biol Chem*, 1995. **270**(42): p. 24674-7.
12. Peserico, A. and C. Simone, Physical and Functional HAT/HDAC Interplay Regulates Protein Acetylation Balance. *Journal of Biomedicine and Biotechnology*, 2011.
13. de Ruijter, A.J., et al., Histone deacetylases (HDACs): characterization of the classical HDAC family. *Biochem J*, 2003. **370**(Pt 3): p. 737-49.
14. Haigis, M.C. and L.P. Guarente, Mammalian sirtuins - emerging roles in physiology, aging, and calorie restriction. *Genes & Development*, 2006. **20**(21): p. 2913-2921.
15. Zimmerman, M. and T. de Lange, 53BP1: pro choice in DNA repair. *Trends in Cell Biology*, 2014. **24**(2): p. 108-117.

16. Zimmermann, M., et al., 53BP1 Regulates DSB Repair Using Rif1 to Control 5' End Resection. *Science*, 2013. **339**(6120): p. 700-704.
17. Escribano-Diaz, C., et al., A Cell Cycle-Dependent Regulatory Circuit Composed of 53BP1-RIF1 and BRCA1-CtIP Controls DNA Repair Pathway Choice. *Molecular Cell*, 2013. **49**(5): p. 872-883.
18. Yim, H., et al., Plk1-mediated stabilization of 53BP1 through USP7 regulates centrosome positioning to maintain bipolarity. *Oncogene*, 2016.
19. Chypre, M., N. Zaidi, and K. Smans, ATP-citrate lyase: A mini-review. *Biochemical and Biophysical Research Communications*, 2012. **422**(1): p. 1-4.
20. Shechter, D., et al., Extraction, purification and analysis of histones. *Nature Protocols*, 2007. **2**(6): p. 1445-1457.
21. Kim, E.Y., et al., Acetylation of malate dehydrogenase 1 promotes adipogenic differentiation via activating its enzymatic activity. *Journal of Lipid Research*, 2012. **53**(9): p. 1864-1876.
22. Kim, W.K., et al., RPTP mu tyrosine phosphatase promotes adipogenic differentiation via modulation of p120 catenin phosphorylation. *Molecular Biology of the Cell*, 2011. **22**(24): p. 4883-4891.

23. Beigneux, A.P., et al., ATP-citrate lyase deficiency in the mouse. *J Biol Chem*, 2004. **279**(10): p. 9557-64.
24. Wakil, S.J., J.K. Stoops, and V.C. Joshi, Fatty acid synthesis and its regulation. *Annu Rev Biochem*, 1983. **52**: p. 537-79.
25. Wang, Q., et al., Abrogation of hepatic ATP-citrate lyase protects against fatty liver and ameliorates hyperglycemia in leptin receptor-deficient mice. *Hepatology*, 2009. **49**(4): p. 1166-75.
26. Berridge, M.J. and R.F. Irvine, Inositol trisphosphate, a novel second messenger in cellular signal transduction. *Nature*, 1984. **312**(5992): p. 315-21.
27. Zhang, W., et al., Essential and redundant functions of histone acetylation revealed by mutation of target lysines and loss of the Gcn5p acetyltransferase. *EMBO J*, 1998. **17**(11): p. 3155-67.
28. Hazzouri, M., et al., Regulated hyperacetylation of core histones during mouse spermatogenesis: involvement of histone deacetylases. *Eur J Cell Biol*, 2000. **79**(12): p. 950-60.
29. Roosen-Runge, E.C., The process of spermatogenesis in mammals. *Biol Rev Camb Philos Soc*, 1962. **37**: p. 343-77.

30. Dai, L., et al., Aberrant levels of histone H3 acetylation induce spermatid anomaly in mouse testis. *Histochemistry and Cell Biology*, 2015. **143**(2): p. 209-224.
31. Karlic, R., et al., Histone modification levels are predictive for gene expression. *Proceedings of the National Academy of Sciences of the United States of America*, 2010. **107**(7): p. 2926-2931.
32. Egloff, S. and S. Murphy, Cracking the RNA polymerase IICTD code. *Trends in Genetics*, 2008. **24**(6): p. 280-288.
33. Zheng, L., et al., Human DNA2 Is a Mitochondrial Nuclease/Helicase for Efficient Processing of DNA Replication and Repair Intermediates. *Molecular Cell*, 2008. **32**(3): p. 325-336.
34. Duxin, J.P., et al., Human Dna2 Is a Nuclear and Mitochondrial DNA Maintenance Protein. *Molecular and Cellular Biology*, 2009. **29**(15): p. 4274-4282.
35. Kleylein-Sohn, J., et al., Plk4-induced centriole biogenesis in human cells. *Developmental Cell*, 2007. **13**(2): p. 190-202.
36. Coelho, P.A., et al., Spindle Formation in the Mouse Embryo Requires Plk4 in the Absence of Centrioles. *Developmental Cell*, 2013. **27**(5): p. 586-597.
37. Quintyne, N.J., et al., Spindle multipolarity is prevented by centrosomal clustering. *Science*, 2005. **307**(5706): p. 127-9.

38. Saunders, W.S., et al., Chromosomal instability and cytoskeletal defects in oral cancer cells. Proc Natl Acad Sci U S A, 2000. **97**(1): p. 303-8.
39. Lau, K.M., et al., Minichromosome maintenance proteins 2, 3 and 7 in medulloblastoma: overexpression and involvement in regulation of cell migration and invasion. Oncogene, 2010. **29**(40): p. 5475-89.
40. Lossaint, G., et al., FANCD2 Binds MCM Proteins and Controls Replisome Function upon Activation of S Phase Checkpoint Signaling. Molecular Cell, 2013. **51**(5): p. 678-690.
41. Thangavel, S., et al., DNA2 drives processing and restart of reversed replication forks in human cells. Journal of Cell Biology, 2015. **208**(5): p. 545-562.
42. Ito, T., et al., A comprehensive two-hybrid analysis to explore the yeast protein interactome. Proc Natl Acad Sci U S A, 2001. **98**(8): p. 4569-74.
43. Zu, X.Y., et al., ATP Citrate Lyase Inhibitors as Novel Cancer Therapeutic Agents. Recent Patents on Anti-Cancer Drug Discovery, 2012. **7**(2): p. 154-167.
44. Lin, R., et al., Acetylation stabilizes ATP-citrate lyase to promote lipid biosynthesis and tumor growth. Mol Cell, 2013. **51**(4): p. 506-18.
45. Donohoe, D.R., et al., The Warburg effect dictates the mechanism of butyrate-mediated histone acetylation and cell proliferation. Mol Cell, 2012. **48**(4): p. 612-26.

46. Ogiwara, H., et al., Histone acetylation by CBP and p300 at double-strand break sites facilitates SWI/SNF chromatin remodeling and the recruitment of non-homologous end joining factors. *Oncogene*, 2011. **30**(18): p. 2135-2146.
47. Bird, A.W., et al., Acetylation of histone H4 by Esa1 is required for DNA double-strand break repair. *Nature*, 2002. **419**(6905): p. 411-5.
48. Das, C., et al., CBP/p300-mediated acetylation of histone H3 on lysine 56 (vol 459, pg 113, 2009). *Nature*, 2009. **460**(7259).
49. Lee, H.S., et al., A cooperative activation loop among SWI/SNF, gamma-H2AX and H3 acetylation for DNA double-strand break repair. *Embo Journal*, 2010. **29**(8): p. 1434-1445.
50. Miller, K.M., et al., Human HDAC1 and HDAC2 function in the DNA-damage response to promote DNA nonhomologous end-joining. *Nature Structural & Molecular Biology*, 2010. **17**(9): p. 1144-U15.
51. Hsiao, K.Y. and C.A. Mizzen, Histone H4 deacetylation facilitates 53BP1 DNA damage signaling and double-strand break repair. *Journal of Molecular Cell Biology*, 2013. **5**(3): p. 157-165.
52. Davie, J.R. and V.A. Spencer, Signal transduction pathways and the modification of chromatin structure. *Prog Nucleic Acid Res Mol Biol*, 2001. **65**: p. 299-340.

53. Wolffe, A.P., Chromatin remodeling: why it is important in cancer. *Oncogene*, 2001. **20**(24): p. 2988-90.
54. Maiorano, D., M. Lutzmann, and M. Mechali, MCM proteins and DNA replication. *Current Opinion in Cell Biology*, 2006. **18**(2): p. 130-136.
55. Bell, S.P. and A. Dutta, DNA replication in eukaryotic cells. *Annu Rev Biochem*, 2002. **71**: p. 333-74.
56. Mendez, J. and B. Stillman, Perpetuating the double helix: molecular machines at eukaryotic DNA replication origins. *Bioessays*, 2003. **25**(12): p. 1158-67.
57. Kang, H.Y., et al., Genetic analyses of *Schizosaccharomyces pombe* dna2(+) reveal that dna2 plays an essential role in Okazaki fragment metabolism. *Genetics*, 2000. **155**(3): p. 1055-67.
58. Liu, Q., W. Choe, and J.L. Campbell, Identification of the *Xenopus laevis* homolog of *Saccharomyces cerevisiae* DNA2 and its role in DNA replication. *J Biol Chem*, 2000. **275**(3): p. 1615-24.
59. Cotta-Ramusino, C., et al., Exo1 processes stalled replication forks and counteracts fork reversal in checkpoint-defective cells. *Mol Cell*, 2005. **17**(1): p. 153-9.
60. Schlacher, K., et al., Double-strand break repair-independent role for BRCA2 in blocking stalled replication fork degradation by MRE11. *Cell*, 2011. **145**(4): p. 529-42.

61. Bettencourt-Dias, M., et al., SAK/PLK4 is required for centriole duplication and flagella development. *Curr Biol*, 2005. **15**(24): p. 2199-207.
62. Habedanck, R., et al., The Polo kinase Plk4 functions in centriole duplication. *Nat Cell Biol*, 2005. **7**(11): p. 1140-6.
63. Rodrigues-Martins, A., et al., Revisiting the role of the mother centriole in centriole biogenesis. *Science*, 2007. **316**(5827): p. 1046-50.
64. Malewicz, M., The role of 53BP1 protein in homology-directed DNA repair: things get a bit complicated. *Cell Death Differ*, 2016. **23**(12): p. 1902-1903.

\*

## ABSTRACT

# **53BP1 regulates histone acetylation through interaction with ATP-Citrate-Lyase**

TingTing Wu

Advisor : Prof. Ho Jin You, Ph.D.

Department of Biomedical sciences,

Graduate school of Chosun University

The tumor suppressor protein 53BP1 functions at the intersection of two major DNA repair pathway promotes non-homologous end joining (NHEJ) and inhibits homologous recombination (HR). Recent many studies show that 53BP1 play a role in different cellular processes.

Here we provide new function of 53BP1, regulating histone acetylation.

We showed that 53BP1 interacts with metabolic enzyme ACL in vitro and vivo, and regulate ACL activity both in cytosolic and nuclear. And found that 53BP1 can regulate ACL ac-

tivity through interaction with ACL. ACL is a cross-link between glucose metabolism and fatty acid synthesis/mevalonate pathway and converts citrate to acetyl-CoA. In the nucleus, acetyl-CoA serves as a substrate for histone acetyltransferases (HATs) that modify histones with acetate to affect the transcription of key metabolism gene.

We identify that through effect on ACL activity, 53BP1 regulate ACL-dependent histone acetylation under different conditions. And based on RNA-sequencing data. 53BP1 deficient cells shown hypoexpression of RNA metabolism relevant genes, DNA repair, cancer, cell death and ROS regulation relevant genes; mtDNA replication and repair relevant gene; centriole biogenesis relevant gene; DNA replication relevant genes and so on, Moreover, acetylation of histone H3 at these genes promoter was specifically reduced upon silencing of 53BP1.

Consequently, 53BP1 through binding with ACL and regulate ACL activity, plays an important role in acetyl-CoA, through regulate histone acetylation, gene expression was changed when slicing of 53BP1. New functions of 53BP1 out in this article.